

OBSERVATIONS FROM EXPERIMENTAL ACID JETTING  
ON LIMESTONE CARBONATES

A Thesis

by

VANESSA CHRISTELLE MPON A NDONHONG

Submitted to the Office of Graduate and Professional Studies of  
Texas A&M University  
in partial fulfillment of the requirements for the degree of

MASTER OF SCIENCE

Chair of Committee,	Ding Zhu
Co-Chair of Committee,	A. Daniel Hill
Committee Member,	Mahmoud El-Halwagi
Head of Department,	A. Daniel Hill

December 2014

Major Subject: Petroleum Engineering

Copyright 2014 Vanessa Christelle Mpon A Ndonhong

## ABSTRACT

Well stimulation is a common practice in petroleum engineering, applied when the production does not meet expectations. Acid jetting is one of the acid stimulation methods, used in carbonate reservoirs where formation damage is present. In acid jetting, an acid solution is “jetted” unto the wellbore surface in the producing zone with the objective of removing the mud filter cake and bypassing the damaged zone by creating wormholes. As for any other stimulation treatments, experimental core studies are performed to get a better understanding of the process and how it can be controlled to achieve successful treatments.

Previous experimental studies have revealed a trend in the experimental results of high velocity acid jetting, namely the formation of a cavity in the vicinity of the injection nozzle, often followed by wormhole propagation from the cavity, throughout the core. These observations have raised the need for a thorough study. For this study, more experiments are run with the objective of qualitatively identify the key parameters affecting the dissolution pattern observed and compare their relative impact. Experiments are conducted on Indiana limestone and Winterset limestone cores of dimension with 15 wt% hydrochloric acid. Different injection rates were used in the experiments, while holding a constant pressure differential across the core, determined from a desired initial interstitial velocity. Permeability values of the cores range from 0.70 mD to 11.50 mD with porosity values between 12% and 25%.

The experimental results show that the key parameters to acid jetting experiments are interstitial velocity across the core, pressure difference across the core, rock permeability, rock heterogeneity and/or pore structure, and acid injection rate. The interstitial velocity across the core appears to be the governing parameter, at all injection rates used. CT scans of the cores after experiments also suggest the existence of optimum conditions for the pressure difference, corresponding interstitial velocity and flux, at which the acid forms a minimal cavity and a less-branched, straight wormhole to breakthrough. These optimum conditions vary with the acid injection rate.

## DEDICATION

This thesis is dedicated to the Almighty God, and my parents, Sara and Joseph.

## ACKNOWLEDGEMENTS

I would like to thank my committee chair, Dr. Zhu, my committee co-chair, Dr. Hill and my committee member, Dr. El-Halwagi, for their guidance and support throughout the course of this research.

Thanks also go to my friends and colleagues and the department faculty and staff for making my time at Texas A&M University a great experience. I also want to extend my gratitude to the Acid Stimulation Research Program and Texas A&M Engineering Experiment Station which provided the funding and experimental support. Thanks to Christopher Holland for teaching me how to run the experiments and to Shangjie Yue for her help with experiments and equipment.

Finally, thanks to all the members of my support system for their encouragement.

## NOMENCLATURE

PI	Productivity Index
q	Flowrate
$\bar{p}$	Average Reservoir Pressure
$p_{wf}$	Flowing Bottomhole Pressure
k	Permeability
h	Formation Thickness
B	Formation Volume Factor
$\mu$	Oil viscosity
$r_e$	Radius of Drainage Area
$r_w$	Wellbore Radius
s	Skin Factor
$k_s$	Permeability of Damaged Zone
$r_s$	Radius of Damaged Zone
$k_v$	Permeability in Vertical Direction
$k_H$	Permeability in Horizontal Direction
$k_{v_s}$	Vertical Permeability of Damaged Zone
$k_{H_s}$	Horizontal Permeability of Damaged Zone
$W_{eff}$	Wormhole Efficiency Factor in the Buijse and Glasbergen Model
$W_B$	Wormhole B-factor in the Buijse and Glasbergen Model
$V_{i-opt}$	Optimum Values of Interstitial Velocity

$PV_{bt-opt}$	Optimum Pore Volume to Breakthrough, Fraction
$PV_{bt}$	Pore Volume to Breakthrough, Fraction
$V_i$	Interstitial Velocity
$Q$	Volumetric Injection Rate
$d_{core}$	Core Diameter
$\phi$	Porosity
$V_{wh}$	Velocity of Wormhole Front
$B(V_i)$	Compact Dissolution Regime at Low Values of $V_i$
$\Delta P$	Corresponding Average Pressure Difference across the Core
$L$	Length of the Core
$D$	Core Diameter
$v$	Injection Velocity
$A$	Cross-section Area of the Core
$m_{saturated}$	Mass of the Fully Saturated Core
$m_{post-jetting}$	Mass of the Core after Acid Jetting Test
$V_{core}$	Bulk Volume of the Core
$V_{acid}$	Total Volume of Acid used during the Jetting Experiment
$\chi$	Volumetric Acid Dissolving Power
$\beta$	Mass Dissolving Power
$\rho_{acid\ solution}$	Density of the Acid Solution
$\rho_{mineral}$	Density of the Mineral
$v_{mineral}$	Species Stoichiometric Coefficient of the Mineral

$v_{acid}$	Species Stoichiometric Coefficient of the Acid
$MW_{mineral}$	Molecular Weight of the Mineral
$MW_{acid}$	Molecular Weight of the Acid
$L_{unstimulated}$	Length of the Unstimulated Zone
$L_{stimulated}$	Length of the Stimulated Zone
$\Delta P_{final}$	Equilibrium Pressure Difference across the Core during the Post-jetting Permeability Test
$\Delta P_{initial}$	Equilibrium Pressure Difference across the Core during the Initial Permeability Test



## TABLE OF CONTENTS

	Page
ABSTRACT .....	ii
DEDICATION .....	iv
ACKNOWLEDGEMENTS .....	v
NOMENCLATURE .....	vi
TABLE OF CONTENTS .....	ix
LIST OF FIGURES.....	xi
LIST OF TABLES.....	xiv
CHAPTER I INTRODUCTION .....	1
I-1 Background On Formation Damage and Well Stimulation.....	1
I-2 Background on Acid Stimulation: Carbonate Acidizing.....	3
I-3 Background on Acid Jetting .....	8
CHAPTER II ACID JETTING EXPERIMENTS.....	15
II-1 Objectives.....	15
II-2 Experimental Setup .....	16
II-3 Experimental Procedure .....	27
II-4 Experimental Design .....	32
II-5 General Laboratory Safety .....	37
CHAPTER III RESULTS AND DISCUSSION .....	40
III-1 Overall Results.....	40
III-2 Effect of Initial Interstitial Velocity.....	42
III-3 Effect of Temperature .....	43
III-4 Effect of Permeability.....	46

III-5 Effect of Porosity or Pore Structure .....	48
III-6 Effect of Pressure Difference across the Core .....	50
III-7 Effect of Acid Injection Velocity.....	52
CHAPTER IV CONCLUSIONS AND RECOMMENDATIONS .....	57
IV-1 Conclusion .....	57
IV-2 Future Studies .....	58
REFERENCES.....	61
APPENDIX A .....	68
APPENDIX B .....	76

## LIST OF FIGURES

FIGURE	Page
1	Illustration of Matrix Acidizing Treatment Outcome in Carbonates (Akanni, 2014) ..... 4
2	Wormhole Efficiency Curve for Indiana Limestone with Corresponding High-Resolution CT Images. (McDuff et al. 2010) ..... 6
3	Core Flood Test Results. Pore Volume to Breakthrough vs Acid Interstitial Velocity (Buijse-Glasbergen, 2005) ..... 8
4	Schematic of Acid Jetting in a Damaged Well (Kalfayan, 2004) ..... 9
5	Acid Jetting Operation in an Openhole Horizontal Well in a Carbonate Reservoir (Mikhailov et al., 2008) ..... 10
6	Rotating Jetting Nozzle (Tempress, 2014) ..... 11
7	Commercial Jetting Nozzle (Limar, 2013) ..... 12
8	Jetting Nozzle Assembly for Acid Tunneling (Portman, 2002) ..... 13
9	3-ft Deep Tunnel Made during 2001 Surface Testing in Indonesia (Stanley, 2010) ..... 14
10	Acid Jetting Experiment General Setup (Holland, 2014) ..... 17
11	Permeability Test Apparatus Schematic (Grabski, 2012) ..... 18
12	Experimental Setup - Core Holder and Fluid Collector System ..... 19
13	Experimental Setup - Acid and Waste Tanks ..... 20
14	Experimental Setup - Water Tank and Injection Pump ..... 21
15	Winterset Limestone Core ..... 22
16	Indiana Limestone Core ..... 22
17	Indiana Limestone from Kocurek Industries(9-mD average permeability) 24

18	Fine Indiana Limestone from Kocurek Industries.....	25
19	Winterset Limestone from Kocurek Industries .....	26
20	Acid Jetting Cavity (Holland 2014) .....	41
21	Effect of Core Temperature on Acid Jetting Experiments at 200ft/s for Low Interstitial Velocity .....	44
22	Acid Jetting for Cores at T=180°F .....	45
23	Acid Jetting at 200ft/sec for Cores with Permeability 9.64mD and 0.76mD.....	47
24	Acid Jetting of Winterset Limestone at 107 ft/sec and $v_i$ of 0.11cm/min..	49
25	Acid Jetting with No Pressure Difference across the Core at 107ft/sec.....	57
26	Acid Jetting at Injection Rates of 150 ft/s and 107ft/s for $V_i$ of 0.14cm/min.....	53
27	Acid Jetting at Injection Rate of 150 ft/s and 107ft/s for $V_i$ of 0.28cm/min and 0.29cm/min.....	55
28	Pressure Difference Observed during Acid Jetting of Core IL05 for 20minutes with No Breakthrough at Injection Velocity of 150 ft/s.....	68
29	Pressure Difference Observed during Acid Jetting of Core IL06 for 15minutes until Breakthrough at Injection Velocity of 150 ft/s.....	69
30	Pressure Difference Observed during Acid Jetting of Core IL07 for 20minutes with No Breakthrough at Injection Velocity of 107ft/sec .....	70
31	Pressure Difference Observed during Acid Jetting of Core IL03 for 17minutes until Breakthrough at Injection Velocity of 107ft/sec .....	71
32	Weight and Pressure Data during Acid Jetting of Core IL05 .....	72
33	Weight and Pressure Data during Acid Jetting of Core IL06 .....	73
34	Weight and Pressure Data during Acid Jetting of Core IL03 .....	74
35	Weight and Pressure Data during Acid Jetting of Core IL07 .....	75

36	Core IL01 CT Scan after Acid Jetting.....	76
37	Core IL02 CT Scan after Acid Jetting.....	77
38	Core IL03 CT Scan after Acid Jetting.....	78
39	Core IL05 CT Scan after Acid Jetting.....	79
40	Core IL06 CT Scan after Acid Jetting.....	80
41	Core IL07 CT Scan after Acid Jetting.....	81
42	Core WS02 CT Scan after Acid Jetting.....	82
43	Core WS03 CT Scan after Acid Jetting.....	83
44	Core WS04 CT Scan after Acid Jetting.....	84

## LIST OF TABLES

TABLE		Page
1	Description of Cores Used for Study .....	23
2	Indiana Limestone Specifications from Kocurek Industries .....	24
3	Winterset Limestone Specifications from Kocurek Industries.....	26
4	Injection Velocity and Corresponding Pump Capacity .....	29
5	Minimum Permeability Values Allowed for Desired Interstitial Velocity and Porosity Values.....	35
6	Effect of Core Temperature on Acid Jetting Experiments at 200ft/s for Low Interstitial Velocity.....	43
7	Acid Jetting for Cores at T=180°F .....	45
8	Acid Jetting at 200ft/sec for Cores with Permeability 9.64mD and 0.76mD.....	46
9	Acid Jetting of Winterset Limestone at 107 ft/sec and $V_i$ of 0.11cm/min	48
10	Acid Jetting with No Pressure Difference across the Core at 107ft/sec.....	50
11	Acid Jetting at Injection Rates of 150 ft/s and 107ft/s for $V_i$ of 0.14cm/min.....	52
12	Injection Rate of 150 ft/s and 107ft/s on Acid Jetting for $V_i$ of 0.28cm/min and 0.29cm/min.....	54
13	Summary of New Experiments Performed at Injection Velocity of 200ft/s	59
14	Summary of New Experiments Performed at Injection Velocity of 150ft/s	59
15	Summary of New Experiments Performed at Injection Velocity of 107ft/s	60

# CHAPTER I

## INTRODUCTION

### I-1 Background on Formation Damage and Well Stimulation

Formation damage is a term which refers specifically to impairments occurring in the near-wellbore region of a well in rock matrix. Formation Damage could be reversed by suitable matrix stimulation treatments. Matrix stimulation is accomplished by injecting a fluid, which could be an acid or a solvent, below the fracturing pressure of the formation (McLeod, 1984). In sandstones, the injection fluid is expected to dissolve and/or disperse materials causing production impairment in sandstones. For carbonates, the fluid will create wormholes, which are flow channels extended into the formation from the wellbore. If properly planned, considerable production improvement can be achieved with matrix stimulation. While the productivity index, PI, is an indicator of well performance, the key parameter to quantify the productivity impairment and the effectiveness of a stimulation treatment is the skin factor “s”. Below is an illustration of how skin factor can be computed and how it correlates with productivity index.

The productivity index of a vertical oil well evaluated at pseudo steady state conditions, with no production impairment is given in field units by

$$PI = \frac{q}{\bar{p} - p_{wf}} = \frac{kh}{141.2B\mu \ln\left(\frac{0.472r_e}{r_w}\right)} \dots\dots\dots(1.1)$$

where  $k$  is the permeability,  $r_e$  is the payzone equivalent radius,  $h$  is the payzone thickness,  $\mu$  is the oil viscosity,  $B$  is the oil formation volume factor and  $r_w$  is the wellbore radius; all in field units.

The Hawkins' formula in equation 1.2 can be used to determine the damage skin effect by assessing the relative effect of permeability impairment and the penetration of damage. In this case the impairment due to damage is reflected as a pressure drop through skin effect, and the resulting damage skin factor can be computed as

$$s = \left( \frac{k}{k_s} - 1 \right) \ln \frac{r_s}{r_w} \dots\dots\dots(1.2)$$

for vertical wells, and

$$s = \left( \frac{k_H}{k_{Hs}} - 1 \right) \ln \left[ \frac{1}{I_{ani}+1} \left( \frac{r_{sH}}{r_w} + \sqrt{\left( \frac{r_{sH}}{r_w} \right)^2 + I_{ani}^2 - 1} \right) \right] \dots\dots\dots(1.3)$$

for horizontal wells, where the subscript  $s$  denotes properties in the damaged region, the subscript  $H$  means horizontal, and  $I_{ani}$  is the anisotropy ratio, defined as the square root of the ratio of the horizontal permeability and the vertical permeability.

The near wellbore region controls productivity; it was observed that damage in this region can significantly decrease production by restricting flow in the formation. Formation damage can be natural or induced. Induced damage results from external factors such as well drilling, completion, workover, stimulation, or injection operation. Natural formation damage is caused by producing reservoir fluid with effects such as fines migration, swelling clays, scales and organic deposits (Hill et al., 2000).

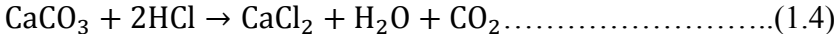
In the field, matrix stimulation treatments with injection below fracture pressure from tubing, drill pipe or coiled tubing usually include a sequence of several fluids,



named stages. A typical minimal treatment schedule will have three stages. The first one is a preflush stage with a non-damaging, non-reactive fluid, until the desired injection rate is achieved. The second stage is the injection of the main treating fluid. The third and last stage is the overflush stage, where the main treatment fluid is cleared out of the tubing and is displaced into the near-wellbore area. (Economides et al., 2013)

I-2 Background on Acid Stimulation: Carbonate Acidizing

An acid matrix treatment is a technique to stimulate wells in order to improve well performance. Hydrochloric acid (HCl) is used for carbonate acidizing because it is highly reactive with calcite and dolomite. The reaction of limestone (calcium carbonate, CaCO<sub>3</sub>) with HCl is:



For dolomite (CaMg(CO<sub>3</sub>)<sub>2</sub>), the reaction is:



In carbonates, formation damage is bypassed to yield new flow channels (wormholes), resulting in a reduced pressure drop (decrease in skin effect). The wormhole configuration is generated because the acid moves in the largest pore throats, vugs and/or fissures and enlarges them. The number of wormholes show a relationship with the pore-size distribution (Schechter and Gidley, 1969). Figure 1 illustrates the matrix acidizing treatment outcome in carbonates for a vertical well.

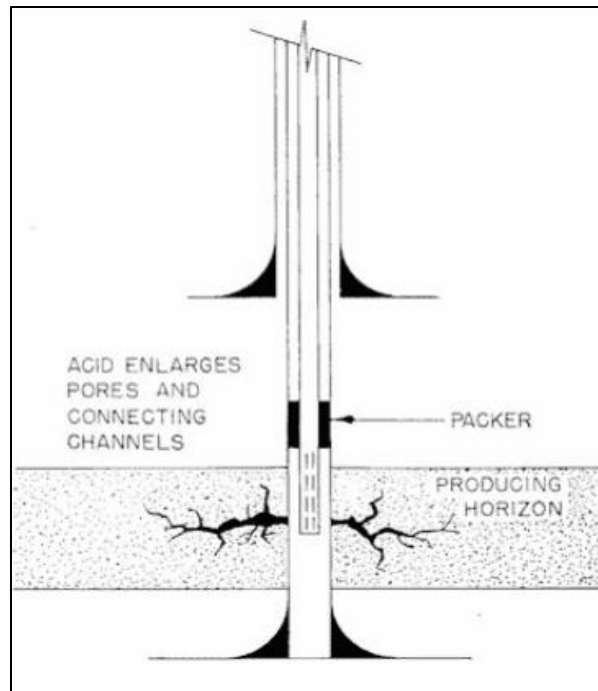


**Figure 1: Illustration of Matrix Acidizing Treatment Outcome in Carbonates (Akanni, 2014)**

In acidizing treatments, the acid solution is injected into the formation below fracture pressure to increase the permeability of carbonates near the wellbore. Formation properties such as permeability and porosity determine the characteristic of fluid flow, as they are continuously altered during acid-rock dissolution.

Acid reaction with carbonate rocks is governed by three mechanisms namely wormhole propagation, compact dissolution and radial flow. At low injection rates, compact dissolution occurs as the formation face is dissolved to enlarge the wellbore. Wormholes start to form when the flow rate is increased to where the Peclet number is approximately 1. The Peclet number of a physical quantity is a dimensionless number

comparing the advection rate to the diffusion rate driven by a gradient. For mass diffusion, the Peclet number is given by

$$Pe = \frac{LU}{D} \dots \dots \dots (1.6)$$

where L is the characteristic length, U is the velocity and D is the mass diffusion coefficient.

When highly reactive fluids are used, the surface dissolution reaction is considered instantaneous and therefore the kinetics of wormhole propagation is dominated by mass-transfer (diffusion), meaning that it depends on how fast the acid is brought in contact with the rock surface. However, if the acidizing fluid flow rate is too fast, the fluid would break through the damaged zone before any wormholes have a chance to form, resulting in a more homogeneous etching pattern. Experiments have established the existence of optimum conditions at which efficient wormholes are formed with the least amount of acid injected, as seen in figure 2.

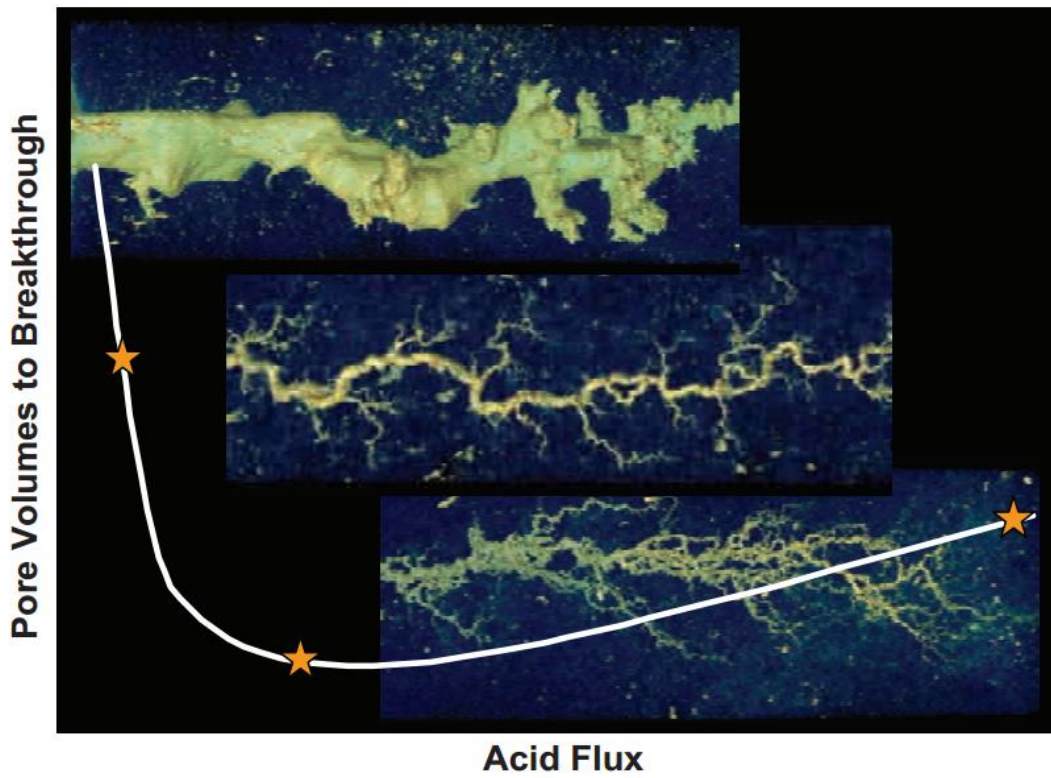


**Figure 2: Wormhole efficiency curve for Indiana limestone with corresponding high-resolution CT images. (McDuff et al. 2010)**

As mentioned in the previous section, the efficiency of the acid treatment is reflected by the change in skin factor, and it has been shown that the type of wormhole has an impact on the skin factor improvement during treatment.

Hung et al. (1989) and Guo et al. (2007) determined that the propagation and structures of the wormholes depend on four main factors: the flow geometry, the injection rate (mass transfer rate), the reaction kinetics, and the fluid loss rate. There are several wormhole propagation models accounting for growth rate, optimum injection

rate and wormhole structure. A notable model is the semi-empirical approach proposed by Buijse and Glasbergen (2005). Here the growth rate of the wormhole front is modeled as a function of interstitial velocity of the acid which itself is a function of acid injection rate. The model is semi-empirical, and parameters such as permeability, mineralogy, temperature and acid concentration are not modeled explicitly. These parameters are rather incorporated in the model in two constants,  $W_{\text{eff}}$  and  $W_B$ , which are determined experimentally from the results of core flood tests. They are determined from the optimum values of interstitial velocity ( $v_{i\text{-opt}}$ ) and pore volume to breakthrough ( $PV_{\text{bt-opt}}$ ) as

$$W_{\text{eff}} = \frac{v_{i\text{-opt}}^{1/3}}{PV_{\text{bt-opt}}} \dots\dots\dots(1.6)$$

$$W_B = \frac{4}{v_{i\text{-opt}}^2} \dots\dots\dots(1.8)$$

and interstitial velocity is,  $v_i$  is defined as

$$v_i = \frac{Q}{\frac{1}{4}\pi d_{\text{core}}^2 \cdot \phi} \dots\dots\dots(1.9)$$

where,  $Q$  is volumetric injection rate in  $\text{m}^3/\text{s}$ ,  $d_{\text{core}}$  is core diameter in  $\text{m}$ ,  $\phi$  is porosity.

The breakthrough pore volume is defined as

$$PV_{\text{bt}} = \frac{v_i}{v_{\text{wh}}} = \frac{v_i^{1/3}}{W_{\text{eff}}B(v_i)} \dots\dots\dots(1.10)$$

where,  $v_{\text{wh}}$  is the velocity of wormhole front in  $\text{m}/\text{s}$ , and the B-function which describes the compact dissolution regime at low values of  $v_i$  is given as

$$B(v_i) = (1 - \exp(-W_B \cdot v_i^2))^2 \dots\dots\dots(1.11)$$

$B(v_i)$  is equal to 1 for  $v_i$  at or above optimum.

Figure 3 shows a typical plot of breakthrough pore volume, PVbt, versus interstitial velocity,  $v_i$ , generated by the Buijse-Glasbergen model.

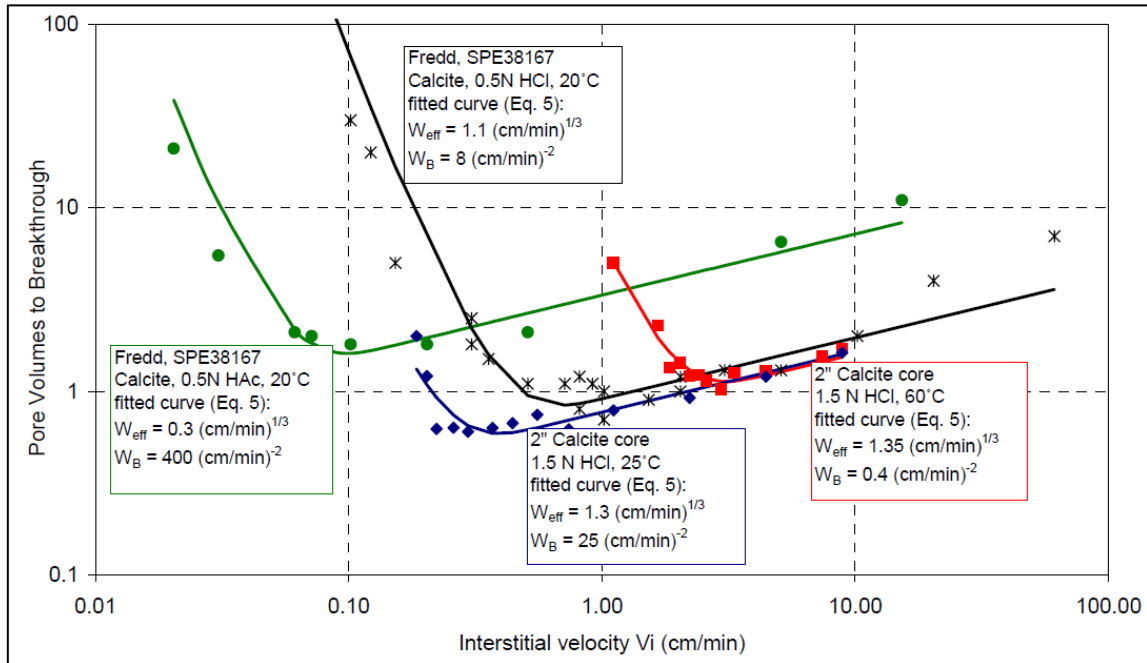


**Figure 3: Core Flood Test Results. Pore Volume to Breakthrough vs Acid Interstitial Velocity (Buijse-Glasbergen, 2005)**

### I-3 Background on Acid Jetting

Acid jetting is a stimulation technique which relies on both mechanical and chemical action between the injection fluid and carbonate rock. It is based on carbonate mechanical integrity and solubility in acids. Acid jetting is the result of a chemical

reaction – dissolution of the carbonate rock in acid, and a mechanical action – injection of high velocity fluids created through high differential pressure orifices. Figure 4 illustrates a jetting procedure.

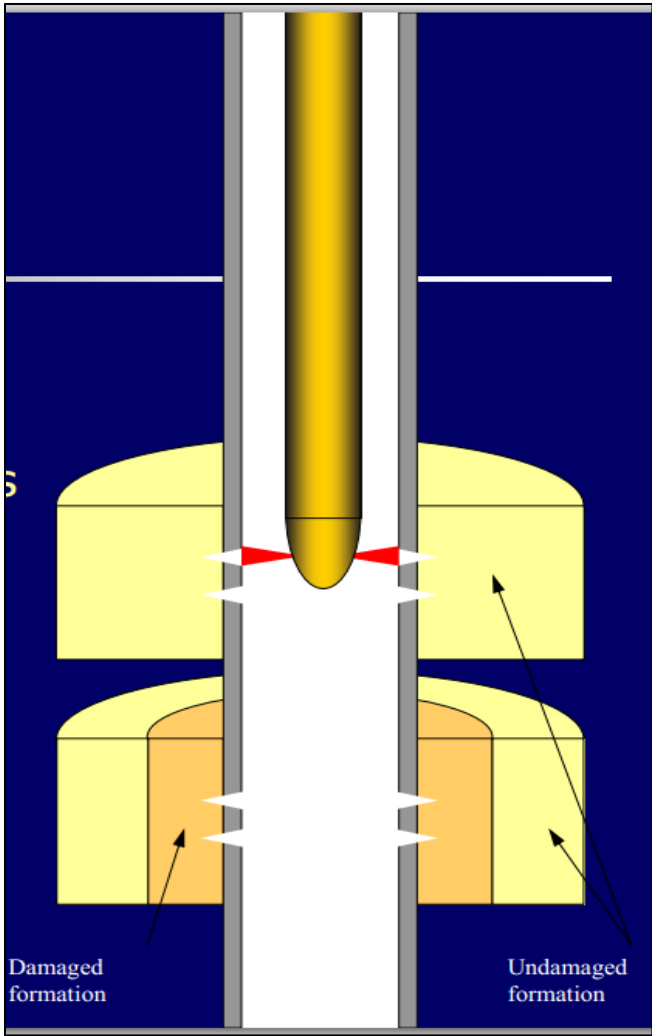


**Figure 4: Schematic of Acid Jetting in a Damaged Well (Kalfayan, 2004)**

Acid jetting is similar to matrix acidizing in that acid is injected below the formation fracture pressure and the wormholes formed could potentially bypass the damage zone (Holland, 2014). Additionally, acid jetting could also accomplish the task of mud filter cake removal, as the high velocity fluid hits the wellbore area (Mikhailov, 2007). The efficiency of the acid jetting treatment, in terms of pore volume to break through, is considerably reduced by the initial formation of a cavity around the injection nozzle, prior to wormhole propagation (Holland, 2014). On the other hand, acid jetting could achieve proper acid placement for matrix stimulation, where thief zones would be avoided and the acid received in the targeted zones (Sasongko, 2012). Figure 5 shows a procedure of jetting in a horizontal well.

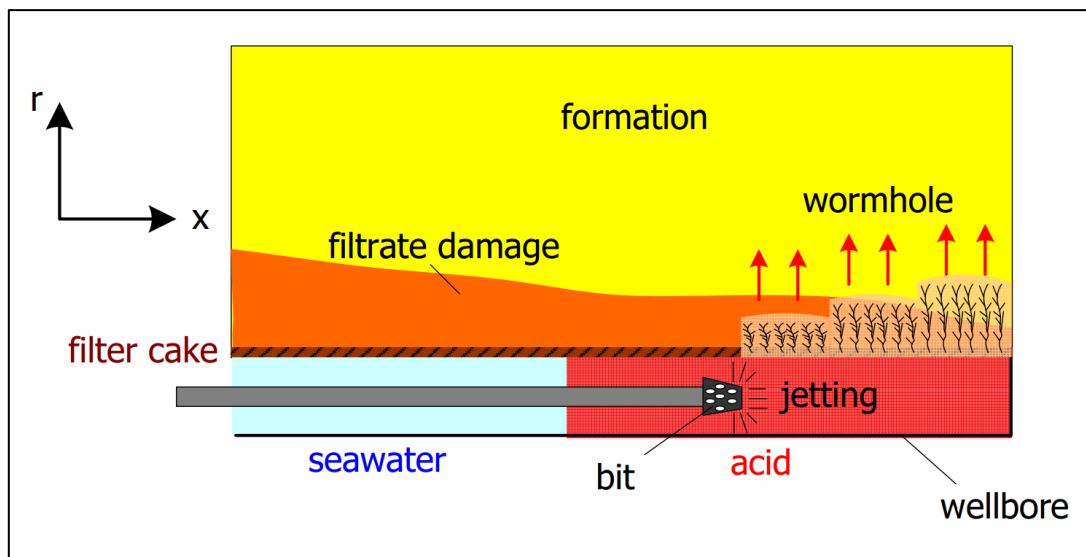


**Figure 5: Acid Jetting Operation in an Openhole Horizontal Well in a Carbonate Reservoir (Mikhailov et al., 2008)**



Regular acid jetting treatments in the field are achieved through coiled tubing, drill pipe or control acid jet. The effectiveness of jetting depends on the stand-off distance, the fluid velocity, the jet stream profile and the pulsation effect from a rotating jet as compared to a stationary jet (Aslam, 2000, Holland, 2014). In the field, a rotary action is required for perforation coverage, as well as screen or openhole coverage.

Figure 6 shows a picture of a rotary jetting nozzle.

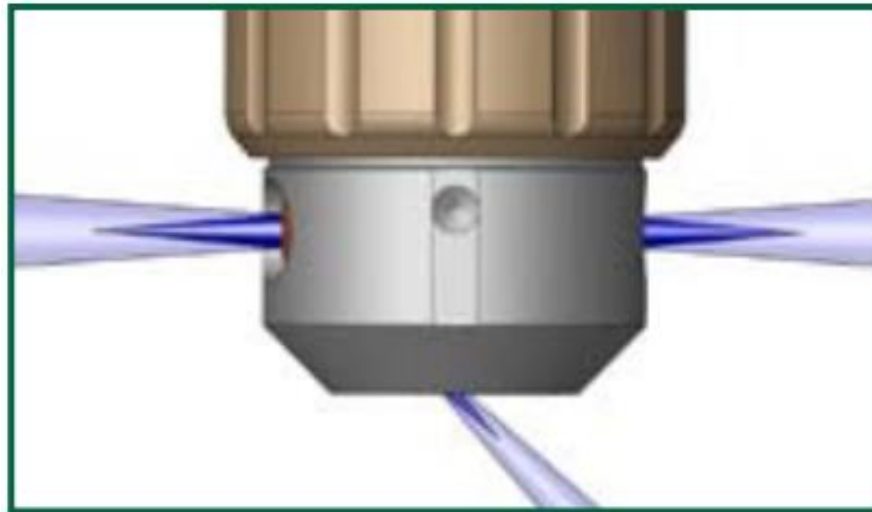


**Figure 6: Rotating Jetting Nozzle (Tempress, 2014)**

Early acid jetting jobs were achieved with simple coiled tubing and a nozzle. These days, more sophisticated methods are available, to achieve larger jobs and reach more complex targets. Figure 7 shows a commercial jetting nozzle designed recently.



**Figure 7: Commercial Jetting Nozzle (Limar, 2013)**

A recent application of acid jetting in carbonates is for a combination of chemical drilling and acid stimulation, called acid tunneling. It is a modified method of the selective stimulation using coiled tubing. The acid tunneling process involves constructing some highly stimulated lateral tunnels in the original well. High permeability drain holes can be constructed in the carbonate formations, without using a drill bit as shown in figure 8 and 9 (Portman et al. 2002). The technique can be used to stimulate horizontal and vertical wells, old or new, injector or producer. This method could provide a greater connectivity to the natural fracture system of the formation and create stable tunnels inside the formation by jetting the acid at high rates using coiled tubing. It could also potentially increase the well drainage area by creating tunnels and creating wormholes in the formation from the tunnels. This process would then bypass the near wellbore region where the damage is to be located (Siddiqui et al., 2013). The very first field application of acid tunneling occurred in 2005 in the Mara field of

Western Venezuela, as an alternative to both initial new well stimulation and producing well maintenance. A considerable and sustained improvement in production was observed (Moss et al. 2006, Rae et al. 2007)



**Figure 8: Jetting Nozzle Assembly for Acid Tunneling (Portman, 2002)**



**Figure 9: 3-ft Deep Tunnel Made during 2001 Surface Testing in Indonesia (Stanley, 2010)**

## CHAPTER II

### ACID JETTING EXPERIMENTS

#### II-1 Objectives

Three related experimental studies were previously performed (Mikhailov, 2007, Zhang, 2009, Holland, 2014). The first and second studies have shown the effect of low velocity water and acid injection on mud filter cake removal and wormhole creation (Mikhailov, 2007, Zhang, 2009). The third study conducted by Holland (2014) initiated an investigation on how high velocity acid injection affects the core's surface and the rock's dissolution pattern. The study also compared the stimulation results between acid jetting and matrix acidizing by comparing the  $PV_{bt-opt}$  and  $v_{i-opt}$  between acid jetting and matrix experiments at similar conditions. The objectives of the current study follow the observations made after all three studies. The purpose will therefore be to:

- 1- Identify the key design parameters in the formation of cavity and wormhole during acid jetting experiments.
- 2- Assess the relative importance of each parameter.
- 3- Initiate a scientific basis to enable future modeling of this process

## II-2 Experimental Setup

The experiment setup is identical to the one used by Holland (2014). Figure 10 provides a schematic of the acid jetting experiment setup.

### II-2-1 Equipment

The experimental apparatus is composed of:

- A pulse pump: Chem/Meter 800 series pulse pump
- A core holder
- A hydraulic pump: Enerpac Co. Model P392 hand pump
- Two back pressure regulators
- A data acquisition system: a pressure transducer, a weight scale, a National Instruments signal processing board and a computer with National Instruments LabView 2012 Software.
- A permeability-measuring device, using a syringe pump, to set a constant flow rate through the core. Figure 11 presents a general schematic of the permeability measurement apparatus setup.
- A time recording system: A timestamp smartphone application and an online computer timer were used to correctly match the pressure and weight data (saved via Labview using the central processing unit's time) with the record of acid injection.

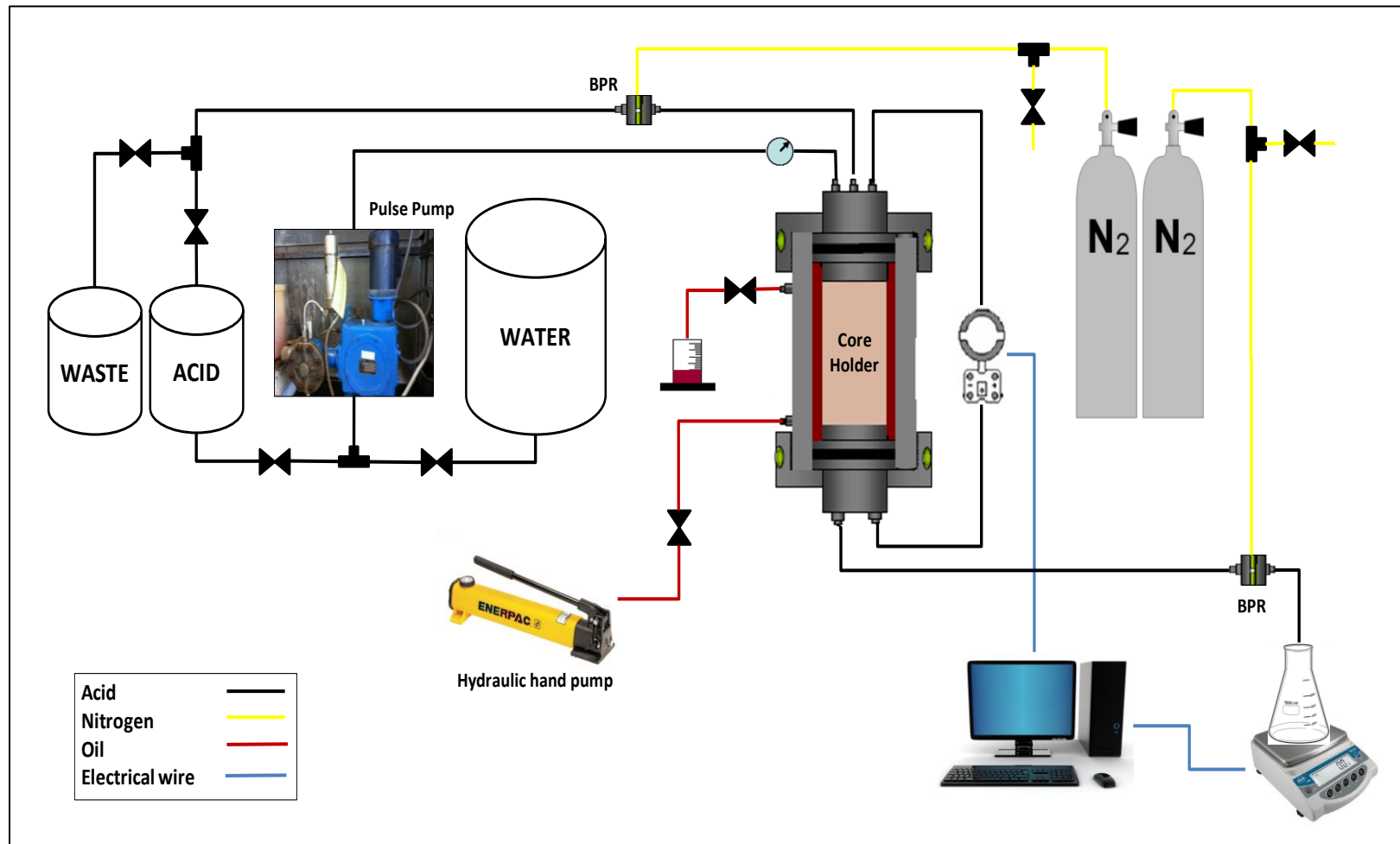


Figure 10: Acid Jetting Experiment General Setup (Holland, 2014)

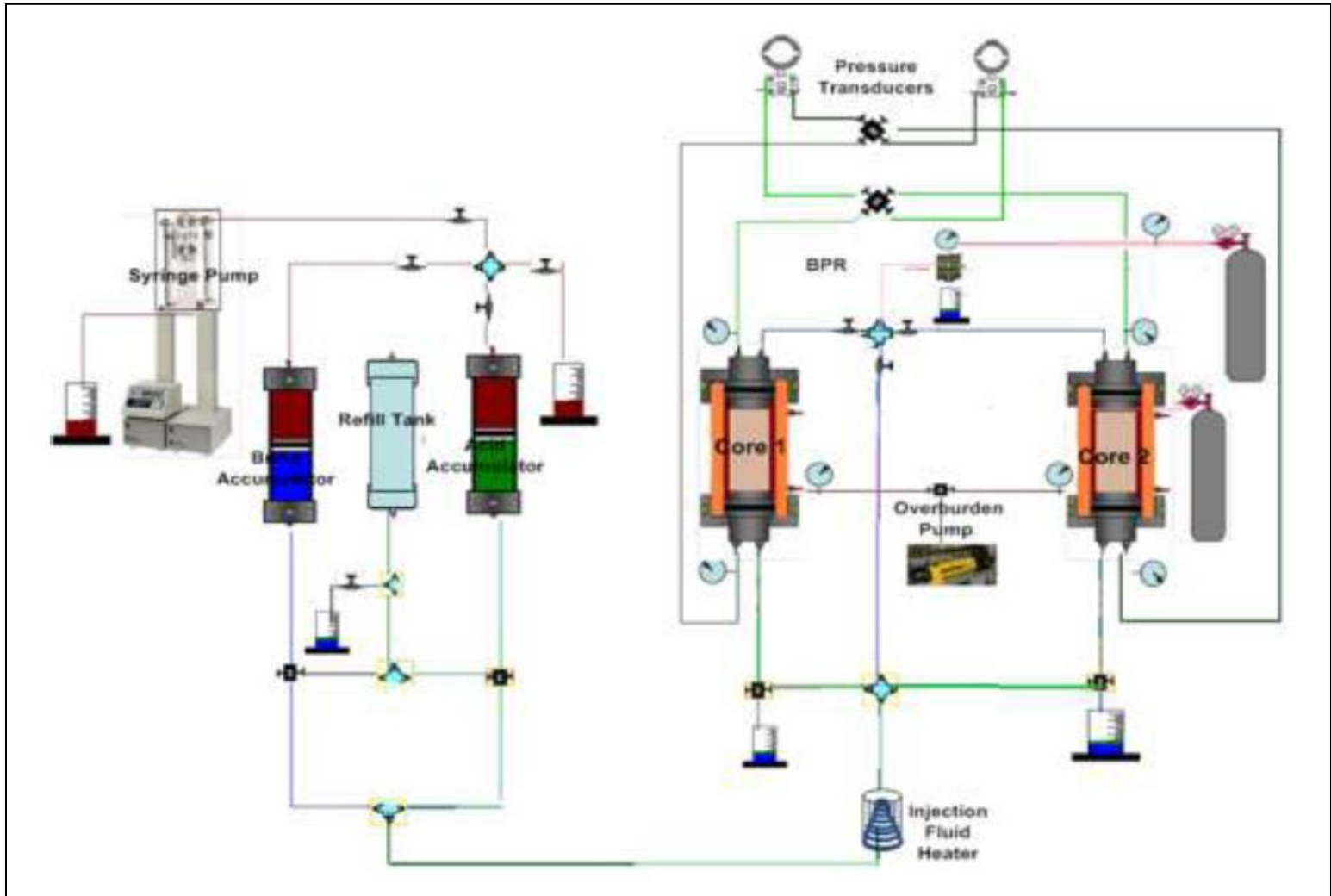


Figure 11: Permeability Test Apparatus Schematic (Grabski, 2012)



A detailed description of the permeability measurement apparatus can be found in Grabski (2012) work.

A detailed description of the acid jetting apparatus can be found in Holland (2014) work. Figure 12, 13 and 14 show the actual setup during acid jetting experiments.



**Figure 12: Experimental Setup - Core Holder and Fluid Collector System**



**Figure 13: Experimental Setup - Acid and Waste Tanks**



**Figure 14: Experimental Setup - Water Tank and Injection Pump**

### II-2-2 Rock Samples

The rock samples used for this study were Winterset limestone cores and Indiana limestone cores. They all were 16 inches in length and 4 inches in diameter. Figure 15 and figure 16 show details of Winterset and Indiana limestone cores respectively. A summary of all the cores used for this study and their properties can be found in Table 1.

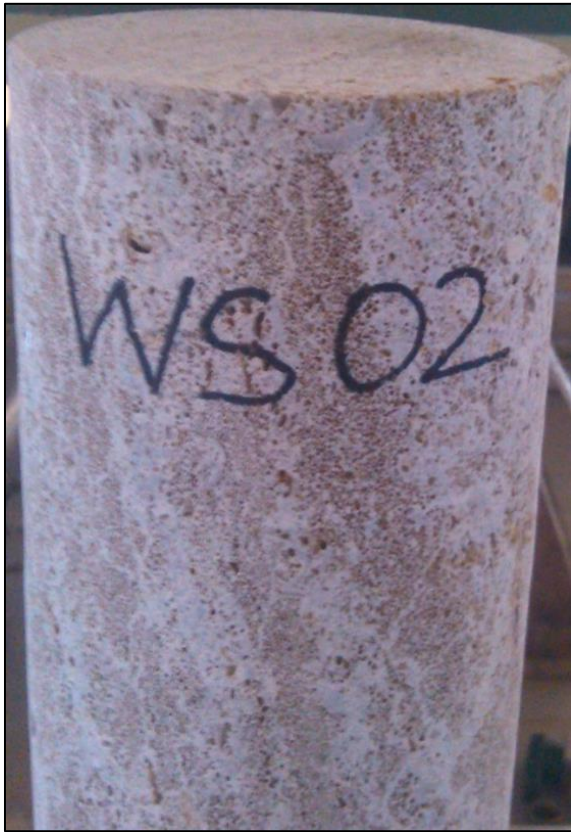


**Figure 15: Winterset Limestone Core**

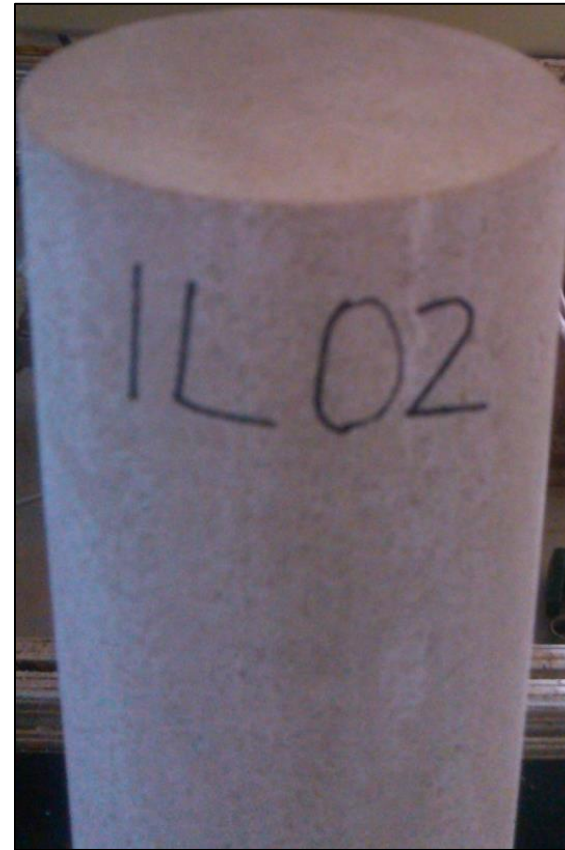


**Figure 16: Indiana Limestone Core**

**Table 1: Description of Cores Used for Study**

Core ID	Type	Permeability (mD)	Porosity (%)	Injection Velocity (ft/sec)
19-IL	Indiana limestone	5.44	15.2	107
20-IL		1.69	12.9	107
21-IL		1.52	14.6	107
23-IL		2.40	15.2	107
IL01		5.86	15.3	150
IL02		9.64	15.7	200
IL03		10.71	15.8	107
IL05		10.50	15.8	150
IL06		11.12	15.8	150
IL07		5.66	15.4	107
WS02	Winterset limestone	0.76	22.42	200
WS03		0.71	23.42	107
WS04		1.00	22.49	107

Limestone is a sedimentary rock dominantly composed of the calcium-bearing carbonate minerals calcite (or calcium carbonate,  $\text{CaCO}_3$ ). Limestone dissolves readily and effervescently in strong acids with the generation of carbon dioxide gas, and the rapidness of the reaction increases with increasing calcite content.

Indiana limestone, a common term for Salem limestone, has been noted to have the highest quality quarried limestone in the United States. It is very homogenous and is

made of approximately 99.9 % calcite. Figure 17 and figure 18 show details of Indiana Limestone cores available from Kocurek industries, with porosity of 18% and 14% respectively, as described in table 2. The permeability of the Indiana limestone cores used ranged from 1mD to about 11mD.

**Table 2: Indiana Limestone Specifications from Kocurek Industries**

Formation	Bedford	Bedford
Permeability	3 mD- Brine Permeability; 9 mD- Gas Permeability	9 mD- Brine Permeability; 17 mD- Gas Permeability
Porosity	14%	18%
Uniaxial Compressive Strength	5,000 psi	5,000 psi
Homogeneous	YES	YES



**Figure 17: Indiana Limestone from Kocurek Industries (9-mD average permeability)**



**Figure 18: Fine Indiana Limestone from Kocurek Industries**

The Winterset limestone cores used had permeability less than 1mD and a porosity of about 23%. Figure 19 shows details of a typical Winterset limestone core available from Kocurek industries with specifications in table 3. Compared to Winterset limestone, the Indiana limestone acid jetting experiment results were more predictable, yet some interesting trends were observed.

**Table 3: Winterset Limestone Specifications from Kocurek Industries**

Formation	Kansas
Permeability	5 mD- Brine Permeability; 15 mD- Gas Permeability
Porosity	19%
Uniaxial Compressive Strength	4,000 psi
Homogeneous	NO

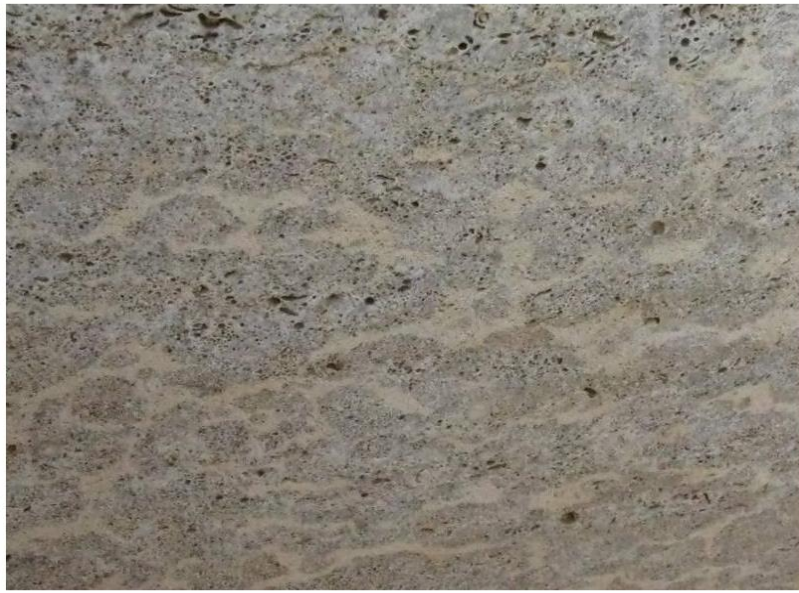


**Figure 19: Winterset Limestone from Kocurek Industries**



Winterset limestone is different from Indiana limestone in terms of rock heterogeneity and response to the acid jetting treatment. It is very porous (~20-25%), yet has a very low permeability (<1md), therefore requiring high pressure differences across the core to achieve steady flow or high interstitial velocities during the experiment. From a geological standpoint, the Winterset limestone is a series of finely crystalline thin-bedded grayish limestone beds separated by shaly siltstone and claystone partings. It also contains calcareous fossil fragments.

### II-2-3 Chemicals

The chemical solution used for this experiment is 15 wt% hydrochloric acid with 0.5 vol% (25mL) of Schlumberger A262 Corrosion Inhibitor. The solution has to be made fresh for each new experiment by diluting the 36.46 wt% HCl solution purchased (Manufactured by Macron Chemical Co.).

### II-3 Experimental Procedure

The experimental procedure can be summarized as follows:

- Label the core following a naming convention established for the study.
- Record the core's dry mass, assuming that the pore space is only occupied by air.
- Saturate the core with water using a vacuum suction pump, which forces water imbibition and air drainage, during eight hours or more.
- Record the core's mass after saturation

- Perform a permeability test, using a syringe pump, with the setup as shown in Figure 11. For more details on the permeability test procedure, please refer to Holland (2014). For more details on the equipment setup for the permeability test, please refer to Grabski (2012).
- Record the core's mass after the permeability test, this mass is expected to be approximately 5% (or less) larger than the recorded weight after saturation, if that is not the case then the future core water saturation time need to be increased accordingly. Also note that the permeability test is much faster when the core is fully water saturated. Therefore, another indication of an inappropriate saturation time is the duration of the permeability test.
- Calculate the core's porosity using the formula below:

$$\phi = \frac{\text{Pore vol.}}{\text{Total vol.}} = \frac{\text{Vol. of fluids forced into the pore space}}{\text{Total vol.}} = \frac{\text{saturated mass} - \text{dry mass}}{\text{fluid density} * \text{total vol.}} \quad (2.1)$$

- Once the core permeability and porosity are determined, given a desired average interstitial velocity, the corresponding average pressure difference across the core is determined as

$$\Delta P = \frac{622.13\mu Lv_i\phi}{k} \dots\dots\dots(2.2)$$

and for a core 16-inches long, we have

$$\Delta P = 9954 \frac{\mu v_i\phi}{k} \dots\dots\dots(2.3)$$

where  $\mu$  is the viscosity in centipoise (cp),  $v_i$  is the interstitial velocity in cm/min,  $L$  is the core length in inches,  $\phi$  is the porosity as a fraction, and  $k$  is the permeability in mD. The interstitial velocity  $v_i$  is defined as:

$$v_i \left( \frac{\text{cm}}{\text{min}} \right) = \frac{q}{A\phi} \dots\dots\dots(2.4)$$

$$A(\text{cm}^2) = \frac{\pi}{4} \left( D \cdot \frac{2.54\text{cm}}{\text{in}} \right)^2 \dots\dots\dots(2.5)$$

$$q \left( \frac{\text{cm}^3}{\text{min}} \right) = \frac{\pi k \left( \frac{D}{4} \right)^2 \Delta P}{96.43\mu\text{L}} \dots\dots\dots(2.6)$$

- Once the average pressure difference across the core is determined, an acid injection velocity is selected and the acid jetting procedure follows. The injection velocity is obtained from the fluid flow rate from the pump, the pump capacity, and the nozzle area as follows:

$$v \left( \frac{\text{ft}}{\text{s}} \right) = \frac{q}{A} \dots\dots\dots(2.7)$$

For a 0.0225 in ID nozzle:

$$A = \frac{\pi}{4} D^2 = \frac{\pi}{4} \left( 0.0225\text{in} \cdot \frac{1\text{ft}}{12\text{in}} \right)^2 = 2.7612 \times 10^{-6} \text{ft}^2 \dots\dots\dots(2.8)$$

$$q \left( \frac{\text{ft}^3}{\text{s}} \right) = 16.3 \frac{\text{gal}}{\text{hr}} \times \text{pump capacity} \times \frac{1 \text{ft}^3}{42 \text{gal}} \times \frac{1 \text{hr}}{3,660 \text{s}} \dots\dots\dots(2.9)$$

The pump capacity is adjusted manually by a micrometer adjustment from 0 to 100%. Table 4 shows corresponding injection velocities and pump capacities.

**Table 4: Injection Velocity and Corresponding Pump Capacity**

Injection velocity (ft/sec)	Pump capacity (%)
100.19	45.75
106.76	48.75
150.01	68.50
200.38	91.50

- The acid jetting process consists of four main stages: the preflush stage with water to establish a constant pressure difference (i.e. constant flux through the

core), the acid preparation stage, the acid injection stage which lasts either twenty minutes or until acid breakthrough, whichever comes first, and the post-treatment flush stage with water to wash-off the acid from the system before stopping.

- After the experiment is completed, the core is taken out of the core holder, further rinsed, then weighed to estimate the bulk volume dissolved during the experiment as follows:

$$\text{bulk volume dissolved} = \frac{(1-\phi)(m_{\text{saturated}} - m_{\text{post-jetting}})V_{\text{core}}}{m_{\text{saturated}}} \dots\dots\dots(2.10)$$

where

$$V_{\text{core}} = \pi L \left(\frac{D}{4}\right)^2 \dots\dots\dots(2.11)$$

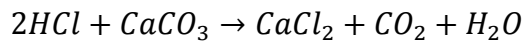
With this value, we use the hydrochloric acid volumetric dissolving power  $\chi$  and mass dissolving power  $\beta$  at the given concentration and temperature assuming constant acid concentration during the experiment to estimate the total volume of acid used. The mineral is assumed to be 100% CaCO<sub>3</sub>. The acid concentration is assumed to remain constant, at the initial concentration, during the experiment.

$$V_{\text{acid}} = \frac{\text{bulk volume dissolved}}{\text{dissolving power}} \dots\dots\dots(2.12)$$

$$\chi = \beta \frac{\rho_{\text{acid solution}}}{\rho_{\text{mineral}}} \dots\dots\dots(2.13)$$

$$\beta = \frac{v_{\text{mineral}} \cdot MW_{\text{mineral}}}{v_{\text{acid}} \cdot MW_{\text{acid}}} \dots\dots\dots(2.14)$$

where  $v$  is the species stoichiometric coefficient in the chemical reaction



where  $v_{HCl}$  equals 2,  $v_{CaCO_3}$  is 1,  $MW_{HCl}$  is the molecular weight of hydrochloric acid and is equal to 36.5 g/mol, and  $MW_{CaCO_3}$  is the molecular weight of calcite and is equal to 100.1 g/mol.

The mass dissolving power for the reaction between pure HCl and  $CaCO_3$  is

$$\beta_{100} = \frac{(1) \cdot (100.1)}{(2) \cdot (36.6)} = 1.37 \frac{gCaCO_3}{gHCl} \dots\dots\dots(2.15)$$

Therefore for 15 wt% HCl we have

$$\beta_{15} = 0.15\beta_{100} = 0.21 \frac{gCaCO_3}{gHCl} \dots\dots\dots(2.16)$$

Since  $\rho_{HCl}$  is 1.07 g/cm<sup>3</sup> and  $\rho_{CaCO_3}$  is 2.71 g/cm<sup>3</sup>

$$\chi_{15} = \beta_{15} \cdot \frac{\rho_{acid\ solution}}{\rho_{mineral}} = 0.21 \frac{gCaCO_3}{gHCl} \left( \frac{1.07 \frac{g}{cm^3}}{2.71 \frac{g}{cm^3}} \right) = 0.0829 \frac{cm^3 CaCO_3}{cm^3 15\%HCl} \dots\dots(2.17)$$

- CT scan the cores to get images of the wormholes inside the core, it also enables us to measure some properties such as volumes and lengths of the observed dissolution patterns in the rock.
- Post-jetting permeability test if the core did not break through to determine the length of the stimulated zone from the relationships below:

$$L_{stimulated} = L - L_{unstimulated} = 16 - L_{unstimulated} \dots\dots\dots(2.18)$$

$$L_{unstimulated} = \Delta P_{final} * \left( \frac{L}{\Delta P_{initial}} \right) \dots\dots\dots(2.19)$$

where,  $\Delta P_{final}$  is the equilibrium pressure difference across the core during the post-jetting permeability test and  $\Delta P_{initial}$  is the equilibrium pressure difference

across the core during the initial permeability test. This length can also be measured directly from the CT scan images,

## II-4 Experimental Design

### II-4-1 Key Parameters

As stated before, one objective is to assess the key parameters in acid jetting with respect to dissolution patterns. For that reason the design of the experiment and the subsequent result analysis have more of a qualitative taste than quantitative. A quantitative analysis will be included for further analysis of this process, as future work. Once the core permeability and porosity are determined, an injection rate and an average interstitial velocity are selected. From the interstitial velocity, a corresponding pressure difference across the core is calculated, based on previous results and expected outcome. Important factors during the acid jetting experiment include the differential pressure behavior, the effluent fluid flow rate behavior and whether or not the acid breaks through the core, and the time for the jetting experiment. More information is obtained after the experiment, especially from the CT scan images.

### II-4-2 Observations

#### a) Constant Pressure differential across the core

It is observed that the set initial differential pressure would fluctuate during the experiment. The fluctuation is more pronounced for larger interstitial velocities. After

the experiment, an average pressure difference over the acid injection period is considered for data analysis. Figure 28 and Figure 29 are respectively pressure responses for IL05 and IL06, both at 150 ft/s acid injection rate from the pump. It is observed that the pressure difference across core IL05 remains steadier than the pressure difference across core IL06. The average interstitial velocity for core IL05 ends up being 0.23cm/min, with no breakthrough (20 minutes of acid injection). For core IL06, the average interstitial velocity is 0.71 cm/min, which is more than twice the initial value and the acid broke through after 15minutes of acid injection.

During the experiment, the variation in pressure difference is also an indication of whether the core would break through or not. Usually when the core is about to breakthrough, we observe a repeated series of slight increase in pressure, then a sharp drop in pressure difference. As soon as breakthrough is observed we should simultaneously switch to water injection and reduce the pressure difference to zero psi to stop the flow of acid in the core and prevent further reactions.

For 107ft/s a similar trend is observed illustrated here by the pressure difference data of core IL03 and core IL07 in figure 30 and figure 31 respectively. Core IL03 has an initial interstitial velocity of 0.21cm/min and an average interstitial velocity of 0.42cm/min after 17 minutes of acid injection. Core IL07 has an initial interstitial velocity of 0.17 cm/min and an average interstitial velocity of 0.20 cm/min after 20minutes of acid injection.

b) Average flux

The flux through the core is observed as the derivative of the effluent fluid accumulation during an experiment. It is observed that it correlates with the pressure difference across the core, therefore it also correlates with the dissolution rate and dissolution pattern inside the core. For low initial interstitial velocities, the flux remains approximately constant which may be observed as the accumulation (mass) is steadily increasing with time at a constant or slightly decreasing rate (straight line or concave down). For higher initial interstitial velocities, the accumulation is increasing at an increasing rate (concave up). Figure 32 and figure 33 show pressure and weight data for core IL05 and core IL06 respectively. The sharp increase in weight observed towards the end is due to acid breakthrough, where the fluid now follows the wormhole path and flows freely through the core.

c) Equipment limitations

- Core dimensions

At this time, the experimental apparatus only allows one core size. The length of the core sample is 16 inches, and the diameter is 4 inches.

- Permeability Requirements and Pressure constraints

The desired interstitial velocity leads to the desired pressure difference across the core, using equation 2.2. It is observed that permeability is inversely proportional to the pressure difference for a set value of interstitial velocity and porosity. Our equipment can currently handle up to 1500 psi of pressure difference across the core holder. For



1500 psi of pressure difference across the core, the minimum core permeability values are found in Table 5.

**Table 5: Minimum Permeability Values Allowed for Desired Interstitial Velocity and Porosity Values**

	$\phi=10\%$	$\phi=15\%$	$\phi=20\%$	$\phi=25\%$
$v_i$ (cm/min)	minimum permeability allowed (mD)			
0.25	0.17	0.25	0.33	0.41
0.5	0.33	0.50	0.66	0.83
1	0.66	1.00	1.33	1.66
1.5	1.00	1.49	1.99	2.49
2	1.33	1.99	2.65	3.32
3	1.99	2.99	3.98	4.98
4	2.65	3.98	5.31	6.64
5	3.32	4.98	6.64	8.30
6	3.98	5.97	7.96	9.95

#### II-4-3 Experiment Results of Importance

##### a) Core Mass Before and After Jetting: Volume of Rock Dissolved

As described in II.3, unlike matrix acidizing, where a known volume of acid is injected into the core at a constant flow rate in an open system, acid jetting is performed under constant pressure in a closed system where the spent acid is recycled back into the system. With the increasing amount of spent acid as the reaction proceeds (especially at high interstitial velocity and/or high pump injection rate), it is observed that the total acid concentration changes during the process, hence discarding the assumption of constant concentration used for stoichiometric considerations to obtain an approximate pore volume to break through.

##### b) Cavity Depth and Volume, Wormhole Length and Density

The major part of the analysis is to study the dissolution pattern following an acid jetting experiment. Generally a cavity forms along the injection path and wormholes initiate from the bottom of the cavity. Depending on the application of the treatment, whether it is for conventional acid jetting or acid tunneling, one will be more interested in the cavity formation, the wormhole propagation or both. Data from the CT scanner enable us to quantify both the cavity properties and the wormhole properties.

##### c) Acid Breakthrough

The experiments are designed for a maximum of 20minutes of acid injection. The experiment is ultimately stopped as soon as we observe acid breakthrough. Achieving

breakthrough is an initial assessment of the effectiveness of the acid treatments, especially combined with the injection time.

d) Pressure Difference across the Core

This measurement correlates with the evolution of the interstitial velocity during the treatment. As explained in the previous sections, a qualitative analysis of the pressure response during the jetting treatment provides an initial assessment of the quality of the treatment. A subsequent quantitative analysis could possibly enable us to model this process.

e) Mass of Effluent (Flux through the Core)

Mass collected at the effluent of the core holder is an accumulative term and it can be translated into an accumulative rate, by a small accumulation increment divided by a small enough time increment. This mass accumulation rate can be converted into a fluid volumetric flow rate by considering a constant density. The fluid volumetric rate is related to the interstitial velocity by equation 2.4.

## II-5 General Laboratory Safety

Only trained and authorized operators are allowed in the laboratory during experiments. Personal protective equipment is mandatory. It includes: close toe shoes,

eye protection, face protection, long pants, lab coat, and gloves when working with acid.

There are three major hazards involved with this experiment.

- Working with High Pressure/ High Temperature Equipment:

The equipment must be leak-proof prior to starting the experiment. All the connections should be checked and double-checked and the loose or worn parts are to be repaired or replaced immediately. Care must also be taken when unfixing connections to do it appropriately to avoid explosions or sudden fluid leaks. Pressures should be raised and released at a slow/controlled pace.

- Working with Heavy Pieces of Equipment:

Appropriate posture should be applied when lifting any large piece of equipment. When lifting the primary parts (core holder, especially with core sample inside), the assumption should be that the piece is heavy and should be handled carefully. The experiment procedure is to be followed carefully without skipping steps.

- Working with Corrosive/Flammable Chemicals:

During the experiments hydrochloric acid and a corrosion inhibitor are used. The handling of these chemicals should always happen under an operating fume hood with the appropriate personal protective equipment. Before every experiment, locate the acid spill kit, the used acid disposal barrel, the eye wash station, and the safety shower station. Ensure that they can be used for the current experiment. If the acid get on the skin or eyes, **immediately** rinse the affected areas with an abundant amount of water for at least 15-20minutes. If acid is splashed onto clothing, remove the clothing immediately, before the acid soaks through the clothing and reacts with the skin. In case

of acid spill, pour the neutralizing solution (pink solution) directly on the spill, then after the neutralization is complete (pink solution turns white) mop the area with plenty of water. After the experiment is complete, carefully dispose of the used acid in the used acid barrel, **do not pour used acid down the drain!!!** Store the fresh acid gallons in a corrosive cabinet, if possible, store it on the bottom shelf. Do not breathe acid fumes, especially when rinsing the graduate cylinders used to prepare the diluted solution.

When preparing the solution, always add acid to water! Never add water to concentrated acid. Slowly add the acid to the water and stir. Chemical splash goggles must be worn whenever acids or acid solutions are used. Safety glasses are not appropriate.

## CHAPTER III

### RESULTS AND DISCUSSION

#### III-1 Overall Results

The overall reaction between hydrochloric acid and calcite rocks comprises three mechanisms: the high velocity injection (mass transfer) of acid on the rock surface, followed by the instantaneous surface reaction of  $\text{H}_3\text{O}^+$  ions and calcite, then the diffusion of the reaction products back to the remainder of the solution. The overall rate determining step is the mass transfer step, as it is slower than the chemical reaction and therefore governs the reaction process. The parameters of interest will therefore be those parameters affecting the mass transfer rate of acid on the rock's surface. These parameters may include: injection rate, fluid flux through the rock's surface (interstitial velocity and pressure difference across the core), permeability, porosity, pore distribution (rock's heterogeneity), calcite content of the core, temperature, acid concentration and injection time.

After going through the acid jetting treatment, the rock samples are scanned to obtain 3-D images of the experimental outcome. For all the rock samples, it was observed that a cavity, usually ball-shaped, formed first, eventually followed by wormholes depending on the experiment conditions.

Holland (2014) compared the depth of the cavity with the injection velocities.

Figure 20 shows a representation of a possible acid flow mechanism during the formation of a cavity.

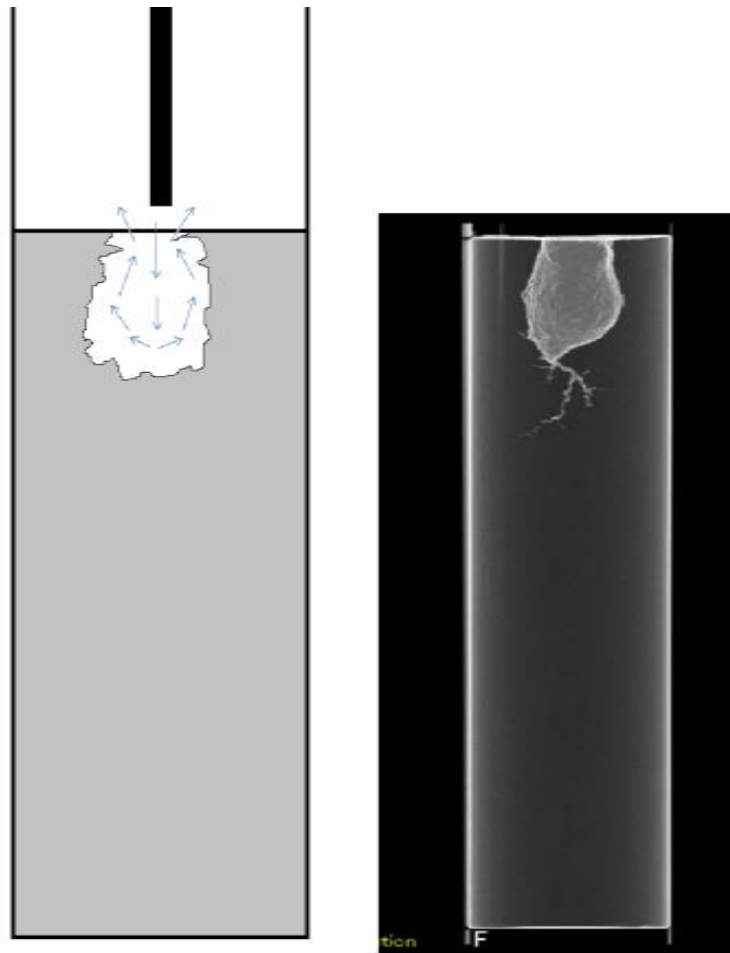


**Figure 20: Acid Jetting Cavity (Holland 2014)**

The current analysis observed a similar trend with the interstitial velocity and total acid injection times. Below or at optimum conditions, the higher the injection rate, the deeper the cavity. For higher interstitial velocities (less than 10min acid injection time to breakthrough), a different behavior is observed. The dominant mechanism is now wormhole formation and propagation and the cavity volume is reduced. This trend indicates the influence of interstitial velocity on both the cavity formation and the wormhole propagation.

The acid jetting mechanism may be considered a mass balance limited transport of fluid in initial turbulent flow through porous media with a chemical reaction at the interface. Parameters such as temperature, injection rate, pressure difference across the core (corresponding to the fluid flux through the core and/or the interstitial velocity), porosity and permeability are determined to be potentially influential in the experimental outcome. The experiment is observed to go through two processes: a cavity formation from the high velocity acid being jetted on the rock surface, and the wormhole propagation.

### III-2 Effect of Initial Interstitial Velocity

The initial interstitial velocity is the actual interstitial velocity that can be measured and adjusted prior to acid injection. Its value is adjusted by changing the pressure difference imposed across the core from the upstream and downstream backpressure regulators and allowing the flow to stabilize. It is achieved during the



initial preflush with water. It is very critical as it determines whether the experiment will be more oriented towards cavity formation, wormhole propagation or a combination of these processes.

### III-3 Effect of Temperature

Three experiments have previously been performed at a core temperature of 180F, two of them used a 15wt% HCl solution and the third one used a 28wt% HCl solution as the injection fluid. The injection fluids were kept at room temperature. Figure 21 and table 6 show the comparison of two acid jetting experiments at different core temperatures and low interstitial velocity. It is observed that the overall dissolution rate increases with temperature, which could be due to a reduction in fluid viscosity. This reduction will improve the diffusion rate of the fluid on the rock surface, as convection is facilitated by the temperature gradient.

**Table 6: Effect of Core Temperature on Acid Jetting Experiments at 200ft/s for Low Interstitial Velocity**

ID	CORE-09-IL	CORE-14-IL
Initial $V_i$ (cm/min)	0.10	0.09
Core Temperature	180 °F	71 °F
Permeability (mD)	3.24	2.08
Porosity (%)	15.43	14.18

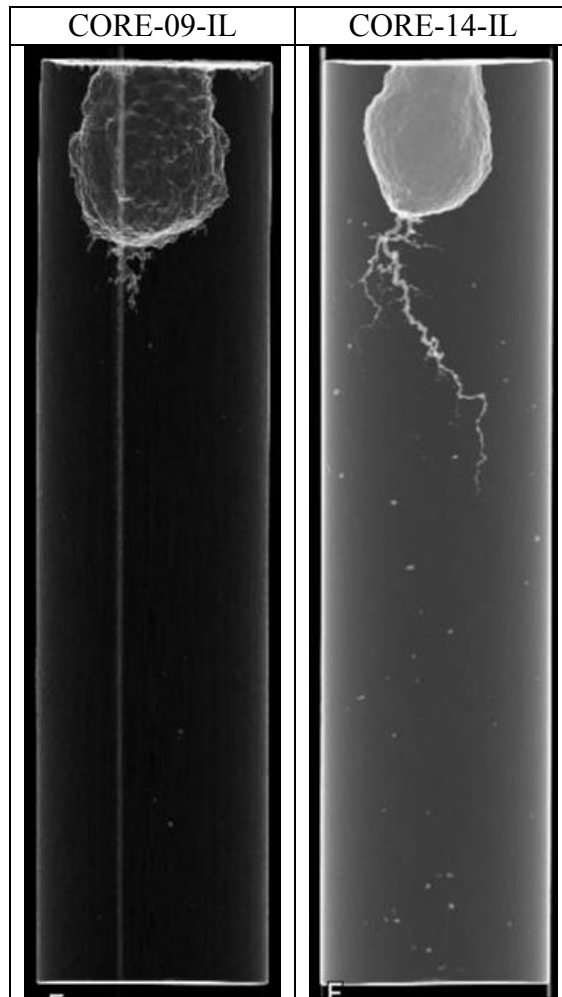


**Figure 21: Effect of Core Temperature on Acid Jetting Experiments at 200ft/s for Low Interstitial Velocity**

Table 7 and figure 22 show a summary of all the experiments run at a core temperature of 180°F. A general observation is that larger and deeper cavities as well as bigger and more branched wormholes are observed, indicating that temperature impacts both the cavity formation and the wormhole propagation mechanisms.

**Table 7: Acid Jetting for Cores at T=180°F**

ID	Core 03-IL	Core 08-IL	Core 09-IL
Initial Vi (cm/min)	0.80	0.24	0.10
Vi_average (cm/min)	1.17	0.51	0.14
HCl wt%	15	28	15
Injection rate (ft/s)	107 (26minutes)	107	200

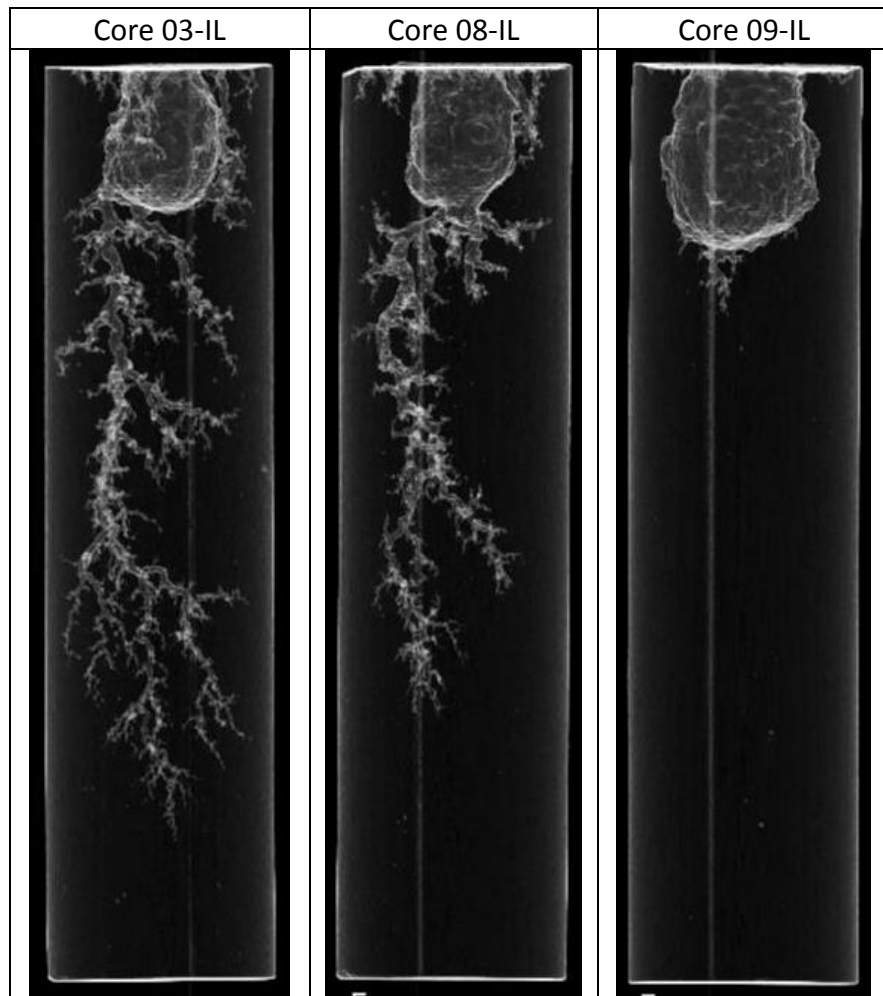


**Figure 22: Acid Jetting for Cores at T=180°F**

### III-4 Effect of Permeability

Permeability is by definition a measure of the ease with which fluid could flow through porous media. It implies that for high permeability cores, one would expect less flow resistance than with low permeability cores. It was observed that permeability has a considerable impact within a specific setting, low pressure difference across the core equivalent to low interstitial velocity. The effect becomes very minor when the initial interstitial velocity and injection velocity get higher as seen in table 8, for injection rate of 200ft/sec.

**Table 8: Acid Jetting at 200ft/sec for Cores with Permeability 9.64mD and 0.76mD**

ID	CORE IL02	CORE WS02
Porosity (%)	15.6	22.42
Permeability (mD)	<b>9.64</b>	<b>0.76</b>
Delta p (psi)	55-65	700-800
Injection time (s)	621	578
Vi_ average (cm/min)	1	0.71
Initial Vi (cm/min)	<b>0.33</b>	<b>0.33</b>
Estimated PVbt assuming 100% calcite	2.23	2.98
Cavity TVD	3.1	2.9

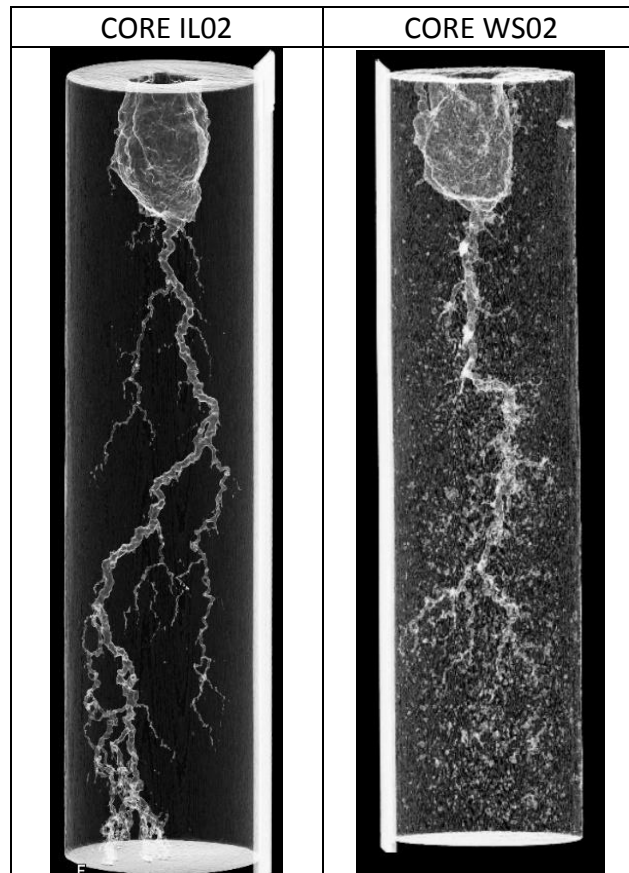


**Figure 23: Acid Jetting at 200ft/sec for Cores with Permeability 9.64mD and 0.76Md**

### III-5 Effect of Porosity or Pore Structure

The porosity has minor impact on the wormhole propagation, as the existence of large pores would form a stable basis for wormhole propagation. The acid may go in the largest pores and react with the matrix surface around it and form a wormhole tip which could propagate following mechanisms presented by Schechter(1992) and Wang (1993). Table 9 and figure 24 show details of two cores with the same initial interstitial velocity and a different dissolution pattern potentially due to the porosity difference.

**Table 9: Acid Jetting of Winterset Limestone at 107 ft/sec and  $v_i$  of 0.11cm/min**

ID	CORE WS03	CORE WS04
Porosity (%)	23.42	22.49
Permeability (mD)	<b>0.71</b>	<b>1.00</b>
Delta p (psi)	180-200	275-290
$V_i$ average (cm/min)	0.16	0.11
Initial $V_i$ (cm/min)	<b>0.11</b>	<b>0.11</b>
Cavity TVD	3.1	2.6

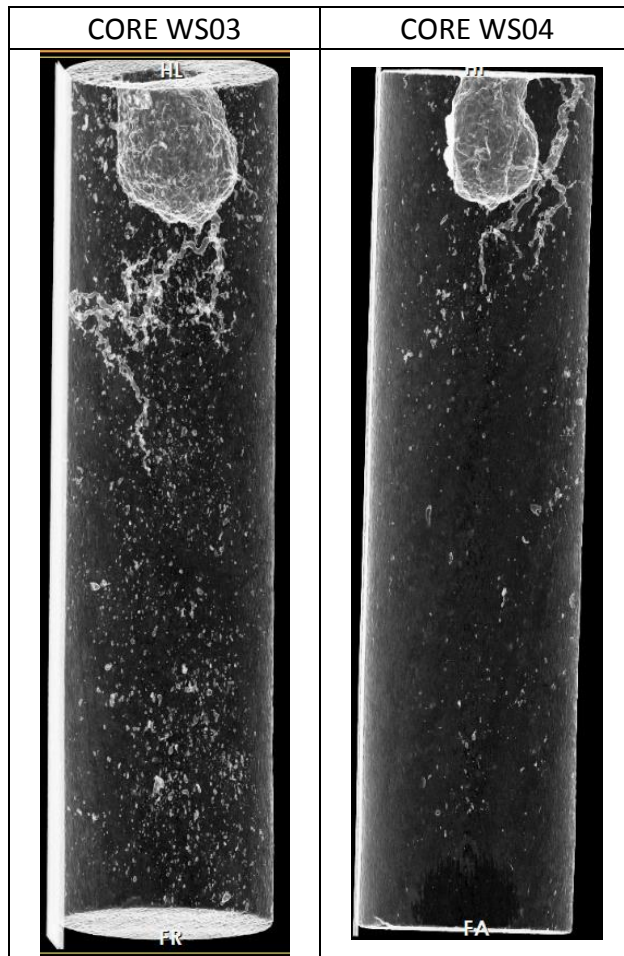


**Figure 24: Acid Jetting of Winterset Limestone at 107 ft/sec and  $v_i$  of 0.11cm/min**

### III-6 Effect of Pressure Difference across the Core

This parameter appears to be one of the governing parameters for the wormhole propagation and it inversely acts on the cavity formation, when coupled with permeability and porosity considerations (interstitial velocity). It is observed that no wormhole forms when there is no flux out of the core and no pressure difference across the core. Table 10 and figure 25 show details of the three experiment results. It is clear that without differential pressure across the core, only cavities form.

**Table 10: Acid Jetting with No Pressure Difference across the Core at 107ft/sec**

ID	Core 19-IL	Core 20-IL	Core 21-IL
Vi (cm/min)	0	0	0
$\Delta P$ (psi)	3.5	0	3.5
k (mD)	5.44	1.69	1.52



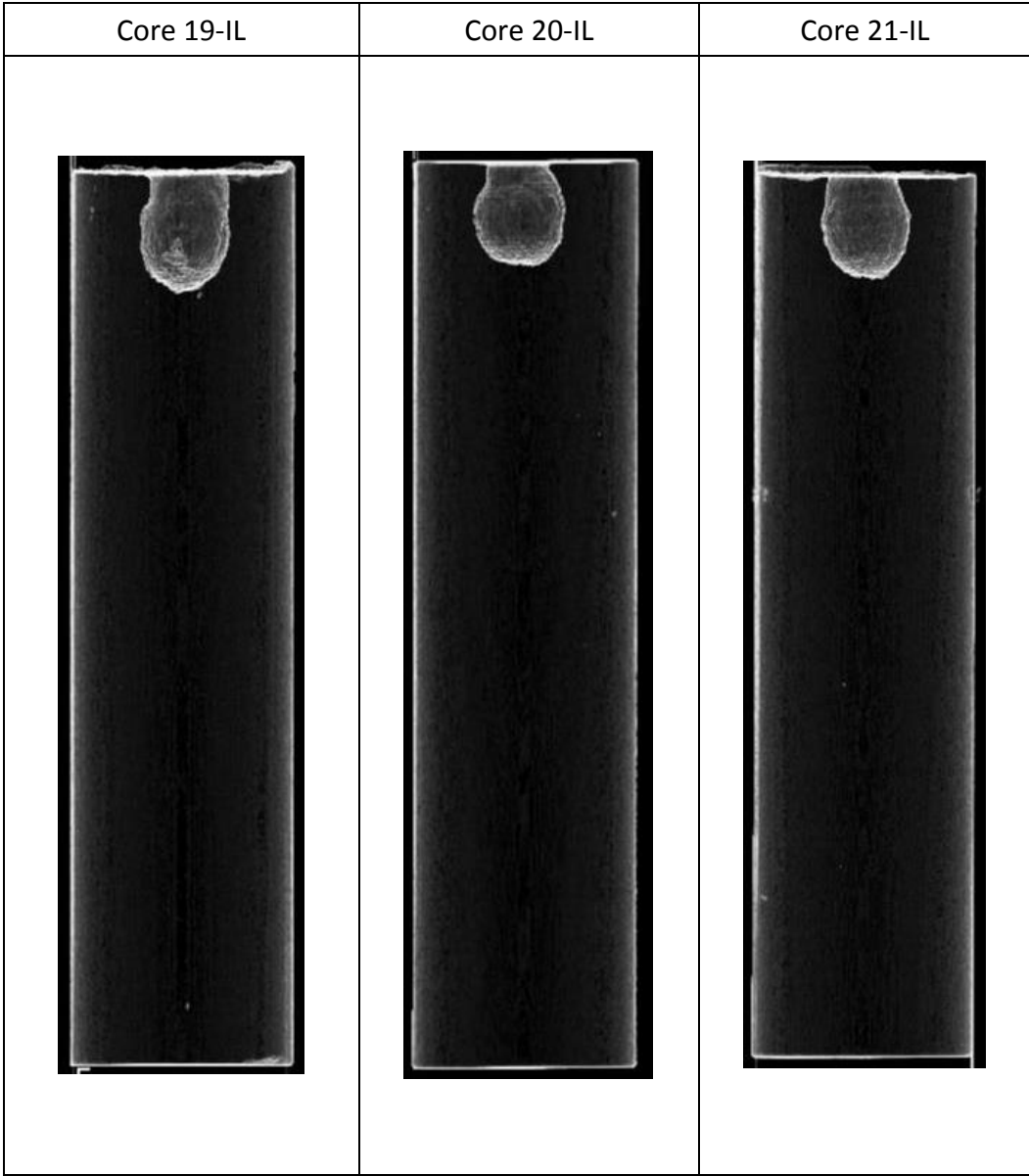


**Figure 25: Acid Jetting with No Pressure Difference across the Core at 107ft/sec**

### III-7 Effect of Acid Injection Velocity

Three injection velocities were used for the experiments: 107ft/sec, 150 ft/sec, and 200ft/ft. It is observed that for low initial interstitial velocities, as the injection velocity increases, the initial interstitial velocity for optimum wormhole propagation increases as well. In other words, a low initial interstitial velocity which would be considered too low for effective wormhole propagation at one injection velocity could lead to an effective wormhole propagation at a lower injection velocity. Table 11 and figure 26 show details of a case where the for the same initial interstitial velocity, we are almost at optimum conditions for 107 ft/sec acid injection, yet the same initial interstitial velocity is well below optimum conditions for 150ft/sec acid injection.

**Table 11: Acid Jetting at Injection Rates of 150 ft/s and 107ft/s for  $V_i$  of 0.14cm/min**

ID	CORE 13-IL	CORE 17-IL
Permeability (mD)	4.48	2.12
Initial $V_i$ (cm/min)	0.14	0.14
Injection time (min)	20	16.3
Injection velocity (ft/s)	150	107



**Figure 26: Acid Jetting at Injection Rates of 150 ft/s and 107ft/s for  $V_i$  of 0.14cm/min**

A different observation is made for higher initial interstitial velocities. In this case, the higher the injection rate the more branching and competing wormholes are observed, regardless of the injection velocity. It means that for high interstitial velocities, a similar dissolution pattern was observed at all acid injection rates, as shown in table 12 and figure 27.

**Table 12: Acid Jetting at Injection Rate of 150 ft/s and 107ft/s for  $V_i$  of 0.28cm/min and 0.29cm/min**

ID	CORE 07-IL	CORE IL06
Permeability (mD)	5.04	11.12
Initial $V_i$ (cm/min)	0.28	0.29
Injection time (min)	12.8	15.8
Injection velocity (ft/s)	200	150

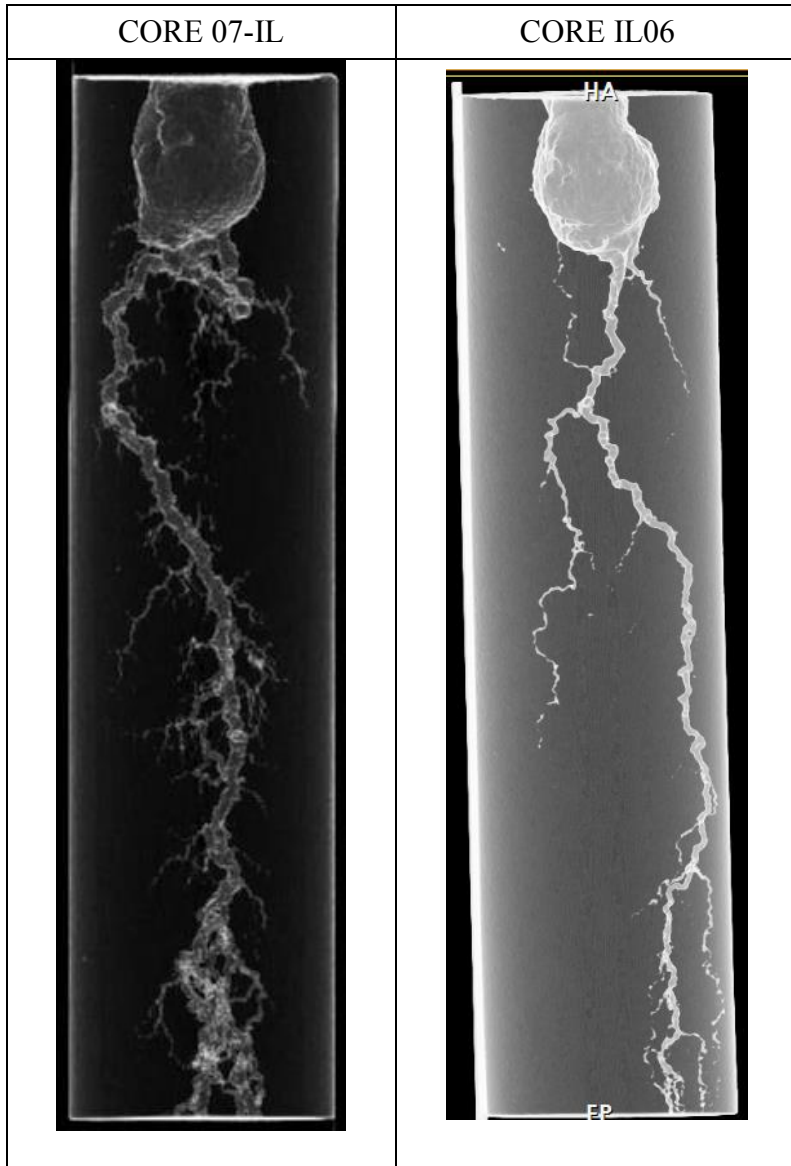


**Figure 27: Acid Jetting at Injection Rate of 150 ft/s and 107ft/s for  $V_i$  of 0.28cm/min and 0.29cm/min**

It is also observed that for low interstitial velocities, presumably below optimum wormhole growth conditions, increasing the injection rate would create deeper cavities. Above the optimum interstitial velocity, as the interstitial velocity increases, the correlation between pump injection velocity and cavity depth becomes weak. This is consistent with the observations by Holland (2014).

## CHAPTER IV

### CONCLUSIONS AND RECOMMENDATIONS

#### IV-1 Conclusion

This study was performed as a continuation of the work by Holland (2014). The objective was to evaluate the effect and importance of various parameters on the results of acid jetting experiments. Experiments are designed for a given desired average interstitial velocity at a specified injection velocity. It was determined that the initial interstitial velocity is the key parameter as it determines the entire experiment's outcome. For a low or intermediate interstitial velocity, the effect of other parameters becomes noticeable. These parameters include core temperature, injection velocity, porosity, permeability and pressure difference across the core. For high interstitial velocities, corresponding to high pressure differences across the core, the injected fluid is forced through the core, hence resulting in a smaller and shorter cavity, and multiple branched wormholes.

The acid jetting mechanism may be considered a mass balance limited transport of fluid in initial turbulent flow through porous media with a chemical reaction at the interface. The relative effect of diffusion and convection are the limiting factors, on the overall reaction since the chemical reaction of carbonates and hydrochloric acid is extremely fast (in the order of nanoseconds)

## IV-2 Future Studies

More experiments will be performed to get a better understanding of the process and confirm or disprove the many hypothesis that are being brought up in the study so far. Cavity and wormhole volumes will be computed from the digital data of the CT scans, to give a better approximation of the PVbt. Some experiments will be run with fixed injection times ( e.g. 5min, 10min and 20min) at high, low and optimum fluxes, regardless of the acid breakthrough, to check for correlations between cavity volume and injection velocity.

After additional experimental work, a theoretical model will be developed to describe the acid jetting process. The experimental results will be the base of the modeling work, and it is expected that the model could be used to predict analytically or semi-empirically the outcome of acid jetting treatments. The transport mechanism will be studied in depth, with considerations for the respective effects of convection and diffusion. Also the cavity formation mechanism and the wormhole will be studied separately and will be later on incorporated as a single coupled process.

The ultimate goal of this project is to produce a work that would find direct application in the field. Therefore it is suggested to consider upscaling the upcoming laboratory scale model to field scale applications. It will include considering different flow geometries (going from linear flow to radial flow) and maybe accounting for the effect of multiple injection points in the wellbore and three dimensional anisotropy.



**Table 13: Summary of New Experiments Performed at Injection Velocity of 200ft/s**

200 ft/sec	phi (%)	k (mD)	Delta p (psi)	Injection time (second)	Vi (cm/min)	Initial vi (cm/min)	Estimated PVbt assuming 100% calcite	Wormhole tip TVD	Cavity TVD	Lwh calculated	k after jetting (mD)
CORE IL02	15.6	9.64	55-65	621	1	0.33	2.23	16	3.1	16	N/A
CORE WS02	22.42	0.76	700-800	578	0.71	0.33	2.98	12.2	2.9	13.89	5.76

**Table 14: Summary of New Experiments Performed at Injection Velocity of 150ft/s**

150 ft/sec	phi (%)	k (mD)	Delta p (psi)	Injection time (second)	Vi (cm/min)	Initial vi (cm/min)	Estimated PVbt assuming 100% calcite	Wormhole tip TVD	Cavity TVD	Lwh calculated	k after jetting (mD)
CORE IL01	15.3	5.86	30-40	1209.9	0.2	0.14	2.85	11.48	3.07	10.15	16.02
CORE IL05	15.61	9.64	30	1202	0.23	0.24	7.98	4.64	2.91	6.91	16.97
CORE IL06	15.77	11.16	45	948	0.71	0.29	2.42	16	2.56	16	N/A

**Table 15: Summary of New Experiments Performed at Injection Velocity of 107ft/s**

107 ft/sec	phi (%)	k (mD)	Delta p (psi)	Injection time (second)	Vi (cm/min)	Initial vi (cm/min)	Estimated PVbt assuming 100% calcite	Wormhole tip TVD	Cavity TVD	Lwh calculated	k after jetting (mD)
CORE 19-IL	15.20	5.44	3.5	1200	0	0	12.36	No wormhole	2.15		
CORE 20-IL	12.90	1.69	0	1200	0	0	3.25		1.84		
CORE 21-IL	14.60	1.52	3.5	1200	0	0	11.93		2.02		
CORE IL03	15.6	10.71	30-41	1056	0.42	0.21	1.45	16	2.28	16	N/A
CORE IL07	15.36	5.58	30	1204	0.2	0.17	4.11	5.70	2.24	5.21	8.28
CORE WS03	23.42	0.71	180-200	1205	0.16	0.11	3.63	7.35	3.11	5.24	1.06
CORE WS04	22.49	1	275-290	1213	0.11	0.11	4.14	3.77	2.59	3.08	1.25

## REFERENCES

- Akanni, T. & Nasr-El-Din, H. Carbonate Matrix Acidizing Models, Class Notes PETE 602 Well Stimulation, Fall 2014, Texas A&M University. College Station, Texas
- Buijse, M.A. and Glasbergen, G. 2005. A Semi-empirical Model to Calculate Wormhole Growth in Carbonate Acidizing. Paper SPE 96892 presented at the SPE Annual Technical Conference and Exhibition, Dallas, Texas, 10/09/2005
- Economides, M.J., Hill, A.D., Ehlig-Economides, C, and Zhu, D. 2013. Petroleum Production Systems, Upper Saddle River, New Jersey: Prentice Hall
- Grabski, E.R. 2012. Matrix Acidizing Core Flooding Apparatus: Equipment and Procedure Description. Master of Science. Texas A&M University. College Station, Texas
- Guo, B., Lyons, W.C., and Ghalambor, A. 2007. Matrix Acidizing in Petroleum Production Engineering, Chapter 16. Burlington: Gulf Professional Publishing.
- Hill, D.G., Lietard, O.M., Piot, B.M. et al. 2000. Formation Damage: Origin, Diagnosis and Treatment Strategy. Reservoir Stimulation, Chapter 14. Third Edition. Wiley Publishing.
- Hung, K.M., Hill, A.D., and Sepehrnoori, K. 1989. A Mechanistic Model of Wormhole Growth in Carbonate Matrix Acidizing and Acid Fracturing. SPE Journal of Petroleum Technology (01). DOI: 10.2118/16886-pa.
- Kalfayan, L.J. 2004. The Art and Practice of Acid Placement and Diversion: History, Present State, and Future. Presentation SPE-108802-DL Distinguished Lecture Series 2004-2005
- Kocurek Industries. 2013. Carbonates Cores, Retrieved on September 29, 2014, from <http://www.kocurekindustries.com/carbonates-cores>
- Limar. 2013. Jetting Nozzles. Retrieved October 01, 2014, from <https://www.limaroiltools.com/coiled-tubing/jetting-nozzles>
- Mikhailov, M. 2007. Acid Placement and Coverage in the Acid Jetting Process. Master of Science. Texas A&M University. College Station, Texas

- Mikhailov, M., Zhu, D. and Hill, A. D. 2008. An Experimental Investigation of Drilling-Fluid Filter-Cake Removal by Acid Jetting. Paper SPE 112373 presented at SPE International Symposium and Exhibition on Formation Damage Control. Lafayette, Louisiana. 13-15 February
- McDuff, D., Jackson, S., Shuchart, C.E., Postl, D. 2010. Understanding Wormholes in Carbonates: Unprecedented Experimental Scale and 3-D Visualization. Paper SPE 129329-JPT Journal of Petroleum Technology, October: 78-81
- Portman, L., Rae, P., and Munir, A. 2002. Full-Scale Tests Prove it Practical to Drill Holes with Coiled Tubing using Only Acid; No Motor, No Bits. Paper SPE-74824 Presented at the SPE/ICoTA Coiled Tubing Conference and Exhibition held in Houston, TX, 9-10 April.
- Schechter, R. S., & Gidley, J. L. 1969. The Change in Pore Size Distribution from Surface Reactions in Porous Media. *AIChE Journal*, 15(3), 339-350.
- Schechter, R.S. 1992. *Oil Well Stimulation*: Prentice Hall. Original edition. ISBN 9780139499340.
- Stanley, F.O., Portman, L.N., Diaz, J.D. et al. 2010. Global Application of Coiled-Tubing Acid Tunneling Yields Effective Carbonate Stimulation. Paper SPE 135604 presented at the SPE Annual Technical Conference and Exhibition held in Florence, Italy, 19-22 September.
- Tempres. 2012. High-Pressure Rotary Jetting Tool. Published in April. Retrieved October 01, 2014, from [http://tempresstech.com/wp-content/uploads/2012/04/HP\\_JBlasting\\_Tool.pdf](http://tempresstech.com/wp-content/uploads/2012/04/HP_JBlasting_Tool.pdf)
- Wang, Y., Hill, A.D., and Schechter, R.S. 1993. The Optimum Injection Rate for Matrix Acidizing of Carbonate Formations. Paper SPE 26578 presented at the SPE Annual technical Conference and Exhibition, Houston, Texas, 10/03/1993
- Zhang, Y. 2009. Experimental Study of Filter Cake Cleanup by Acid/Water Jetting. Master of Science. Texas A&M University. College Station, Texas

### Supplemental Sources:

- Albertson, M.L., Dai, Y.B., Jensen, R.A. and Rouse, H. Diffusion of Submerged Jets. ASCE Paper 2409. December, 1948.
- Aslam, J. and Al Salat, T. 1998. Stimulation of Horizontal Wells in Carbonate Reservoirs. Paper SPE 49493 presented at Abu Dhabi International Petroleum Exhibition and Conference, Abu Dhabi, U.A.E., 10/11/1998
- Aslam, J. and Al Salat, T. 2000. High-Pressure Water Jetting: An Effective Method to Remove Drilling Damage. Paper SPE 58780 presented at SPE International Symposium on Formation Damage Control. Lafayette, Louisiana. 02/23/2000
- Buijse, M.A. 2000. Understanding Wormholing Mechanisms Can Improve Acid Treatments in Carbonate Formations. SPE Production & Operations 15 (3): 168-175.
- Churcher, P.L., French, P.R., Shaw, J.C. and Schramm, L.L. 1991. Rock Properties of Berea Sandstone, Baker Dolomite, and Indiana Limestone. Paper SPE 21044 presented at SPE International Symposium on Oilfield Chemistry. Anaheim, California. 02/20/91
- Cinco, H., Miller, F. G., & HJ, R. 1975. Unsteady-state pressure distribution created by a directionally drilled well. Journal of Petroleum Technology, 27(11), 1392-1400.
- Daccord, G., Touboul, E., & Lenormand, R. (1989). Carbonate Acidizing: Toward a Quantitative Model of the Wormholing Phenomenon. SPE production engineering, 4(1), 63-68.
- Dresser, Inc. 2014. Mity Mite back pressure regulator.  
[http://www.dresser.com/documents/RedQ/regulator\\_broc\\_redq\\_spec\\_reg\\_brochure\\_f.pdf](http://www.dresser.com/documents/RedQ/regulator_broc_redq_spec_reg_brochure_f.pdf). Downloaded 08 January 2014
- Equilibar Precision Control. 2014. Equilibar back pressure regulator.  
<http://www.equiblar.com/PDF/research-back-pressure-regulators.pdf>. Downloaded 08 January 2014
- Economides, M., Deimbachor, F.X., Brand, C.W. et al. 1991. Comprehensive Simulation of Horizontal-Well Performance. SPE Formation Evaluation 6 (4): 418-426. DOI: 10.2118/20717-pa
- Economides, M.J. and Boney, C. 2000. Reservoir Stimulation in Petroleum Production. Reservoir Simulation. M.J. Economides and K.G. Nolte (eds), John Wiley & Sons, New York City.

- Enerpac. 2014. Instruction Sheet – Hydraulic Hand Pumps.  
[http://www.enerpac.com/sites/default/files/11763\\_i\\_3.pdf](http://www.enerpac.com/sites/default/files/11763_i_3.pdf). Downloaded 12  
January 2014
- Fatt, I. 1956. The Network Model of Porous Media. I, II, III. *Pet. Trans. AIME*, 207,  
144.
- Fredd, C.N. 2000. Dynamic Model of Wormhole Formation Demonstrates Conditions  
for Effective Skin Reduction During Carbonate Matrix Acidizing. Paper SPE  
59537 be presented at the SPE Permian Basin Oil and Gas Recovery Conference.  
Midland, Texas, 21-23 March.
- Fredd, C.N. and Fogler, H.S. 1998. Influence of Transport and Reaction on Wormhole  
Formation in Porous Media. *American Institute of Chemical Engineers. AIChE  
Journal* 44 (9): 1933.
- Fredd, C.N. and Fogler, H.S. 1999. Optimum Conditions for Wormhole Formation in  
Carbonate Porous Media: Influence of Transport and Reaction. *SPE Journal* 4  
(3): 196-205
- Fredd, C.N. and Miller, M.J. 2000. Validation of Carbonate Matrix Stimulation Models.  
Paper presented at the SPE International Symposium on Formation Damage  
Control, Lafayette, Louisiana. 2000, Society of Petroleum Engineers Inc  
00058713. DOI: 10.2118/58713-ms.
- Frick, T.P., Kurmayr, M., and Economides, M.J. 1994. Modeling of Fractal Patterns in  
Matrix Acidizing and Their Impact on Well Performance. *SPE Production &  
Operations* 9 (1): 61-68.
- Furui, K., Burton, R., Burkhead, D., Abdelmalek, N., Hill, A., Zhu, D., & Nozaki, M.  
2012. A Comprehensive Model of High-Rate Matrix-Acid Stimulation for Long  
Horizontal Wells in Carbonate Reservoirs: Part I--Scaling Up Core-Level Acid  
Wormholing to Field Treatments. *SPE Journal*, 17(1), 271-279.
- Gdanski, R. 1999. A Fundamentally New Model of Acid Wormholing in Carbonates.  
Paper SPE 54719 presented at the SPE European Formation Damage Conference,  
Netherlands, 31 May – 01 June.
- Glasbergen, G., Kalia, N., and Talbot, M.S. 2009. The Optimum Injection Rate for  
Wormhole Propagation: Myth or Reality? Paper SPE 121464 presented at the 8th  
European Formation Damage Conference, Scheveningen, 27 – 29 May.

- Golfier, F., Zarcone, C., Bazin, B., Lenormand, R., Lasseux, D., and Quintard, M. 2002. On The Ability of a Darcy-Scale Method Model to Capture Wormhole Formation During the Dissolution of a Porous Medium. *J. Fluid Mech.*, 457,213.
- Gong, M, and A.M. El-Rabba. 1999. Quantitative model of wormholing process in carbonate acidizing. Paper SPE 52165 presented at the Mid-Continent Operations Symposium, Oklahoma City, Oklahoma, 18-21 February.
- Hansen, J.H. and Nederveen, N. 2002. Controlled Acid Jet (CAJ) Technique for Effective Single Operation Stimulation of 14,000+ ft Long Reservoir Sections. Paper SPE 78318 presented at the 13<sup>th</sup> European Petroleum Conference, Aberdeen, Scotland, U.K. 10/29/2002
- Hoefner, M.L. and Fogler, H.S. 1988. Pore Evolution and Channel Formation During Flow and Reaction in Porous Media. *AIChE Journal* 34 (1): 45-54.
- Hoefner, M.L. and Fogler, H.S. 1989. Fluid-Velocity and Reaction-Rate Effects During Carbonate Acidizing: Application of Network Model. *SPE Production Engineering* (02) DOI: 10.2118/15573-pa.
- Holland, C.C. 2014. Experimental High Velocity Acid Jetting in Limestone Carbonates. Master of Science. Texas A&M University. College Station, Texas
- Hoefner, M.L. and Fogler, H.S. 1989. Fluid-Velocity and Reaction-Rate Effects During Carbonate Acidizing: Application of Network Model. *SPE Production Engineering* (02) DOI: 10.2118/15573-pa.
- Huang, T., Hill, A.D., and Schechter, R.S. 1997. Reaction Rate and Fluid Loss: The Keys to Wormhole Initiation and Propagation in Carbonate Acidizing. Paper SPE 37312 presented at the International Symposium on Oilfield Chemistry, Houston, Texas, 18 –21 February.
- Huang, T., Zhu, D., and Hill, A.D. 1999. Prediction of Wormhole Population Density in Carbonate Matrix Acidizing. Paper presented at the SPE European Formation Damage Conference, The Hague, Netherlands. Copyright 1999, Society of Petroleum Engineers, Inc. 00054723. DOI: 10.2118/54723-ms.
- Jin, Xiao. 2013, Experimental Investigation for the Effects of the Core Geometry on the Optimum Acid Flux in Carbonate Acidizing. Master of Science. Texas A&M University. College Station, Texas
- Kalia, N., & Balakotaiah, V. (2009). Effect of Medium Heterogeneities on Reactive Dissolution of Carbonates. *Chemical Engineering Science*, 64(2), 376-390.

- Kalia, N. and Balakotaiah, V. 2007. Modeling and Analysis of Wormhole Formation in Reactive Dissolution of Carbonate Rocks. *Chemical Engineering Science* 62 (4): 919-928.
- Karakas, M., & Tariq, S.M. (1991). Semianalytical Productivity Models for Perforated Completions. *SPE Production Engineering*, 6(1), 73-82.
- Kuchuk, F.J., Goode, P.A., Brice, B.W. et al. 1990. Pressure-Transient Analysis for Horizontal Wells. *Journal of Petroleum Technology* 42(8): 974-979, 1028-1031. DOI: 10.2118/18300-pa
- Lefevre, M. J. First Aid Manual for Chemical Accidents, 2nd Ed. Van Nostrand Reinhold: New York, 1989.
- Liu, M., Zhang, S., and Mou, J. 2012. Effect of Normally Distributed Porosities on Dissolution Pattern in Carbonate Acidizing. *Journal of Petroleum Science and Engineering* 94–95 (0): 28-39.
- Liu, X., Ormond, A., Bartko, K. et al. 1997. A Geochemical Reaction-Transport Simulator for Matrix Acidizing Analysis and Design. *Journal of Petroleum Science and Engineering* 17 (1–2): 181-196.
- Maheshwari, P., Ratnakar, R. R., Kalia, N., & Balakotaiah, V. 2012. 3-D Simulation and Analysis of Reactive Dissolution and Wormhole Formation in Carbonate Rocks. *Chemical Engineering Science*.
- McDuff, D., Shuchart, C.E., Jackson, S., Postl, D., Brown, J.S. et al. 2010. Understanding Wormholes in Carbonates: Unprecedented Experimental Scale and 3-D Visualization. Paper SPE 134379 presented at the SPE Annual 77 Technical Conference and Exhibition, Florence, Italy, 09/19/2010. doi: 10.2118/134379-ms
- Pekarek, J. L., Lowe, D. K. and Huitt, J. L. 1963. Hydraulic Jetting – Some Theoretical and Experimental Results. Paper SPE 421.
- Panga, M.K.R., Ziauddin, M., and Balakotaiah, V. 2005. Two-Scale Continuum Model for Simulation of Wormholes in Carbonate Acidization. *AIChE Journal* 51 (12): 3231- 3248.
- Panga, M., Ziauddin, M., Gandikota, R., & Balakotaiah, V. 2004. A New model for Predicting Wormhole Structure and Formation in Acid Stimulation of Carbonates. Paper SPE 86517 presented at the SPE International Symposium and Exhibition on Formation Damage Control. Lafayette



- Ritchie, B., Abbasy, I., Pitts, M., White, B. and Rushdun Jaafar, M. 2008. Challenges in Completing Long Horizontal Wells Selectively. Paper SPE 116541 presented at SPE Asia Pacific Oil and Gas Conference and Exhibition, Perth, Australia. 10/20/2008
- Scope Production Developments. 2014. Spincat  
<http://www.scopeproduction.com/spincat.php>. Downloaded 08 January 2014
- Siddiqui, M.A., Sharma, S.S., Al-Ajmi, M.F. et al. 2013. Enhance of Oil Production from an Old Well in Thin Carbonate Reservoir through Acid Tunneling – A Case Study. Paper SPE 164876 presented at the EAGE Annual Conference & Exhibition incorporation SPE Europe held in London, UK, 10-13 June.
- Simon, R., and Kelsey, F. J. 1972. The Use of Capillary Tube Networks in Reservoir Performance Studies. I, II. Soc. Pet. Eng. J., 99, 345.
- Smith, C.F., Dollarhide, F.E., and Byth, N.J. 1978. Acid Corrosion Inhibitors - Are We Getting What We Need? Journal of Petroleum Technology 30 (5): 737-746. DOI: 10.2118/5644-pa
- Steere, N. V. 1971. CRC Handbook of Laboratory Safety. Second Edition, CRC: Boca Raton
- Taylor, K.C., Al-Ghamdi, A.H., and Nasr-El-Din, H.A. Effect of Additives on the Acid Dissolution Rates of Calcium and Magnesium Carbonates. SPE Prod & Fac. August 2004.
- Teikoku USA Inc Chempump. 2014. Chem/Meter 800 Series  
[http://www.chempump.com/images/technical\\_literature/chem\\_meter/brochures/800series-02.pdf](http://www.chempump.com/images/technical_literature/chem_meter/brochures/800series-02.pdf). Downloaded 08 January 2014
- Thompson, K. E., & Fogler, H. S. 1997. Modeling Flow in Disordered Packed Beds from Pore-Scale Fluid Mechanics. AIChE Journal, 43(6), 1377-1389.
- Yildiz, T. 2000. Assessment of total skin factor in perforated wells. SPE Reservoir Evaluation & Engineering, 9(1), 61-76.

APPENDIX A

PRESSURE AND WEIGHT DATA DURING ACID JETTING EXPERIMENTS

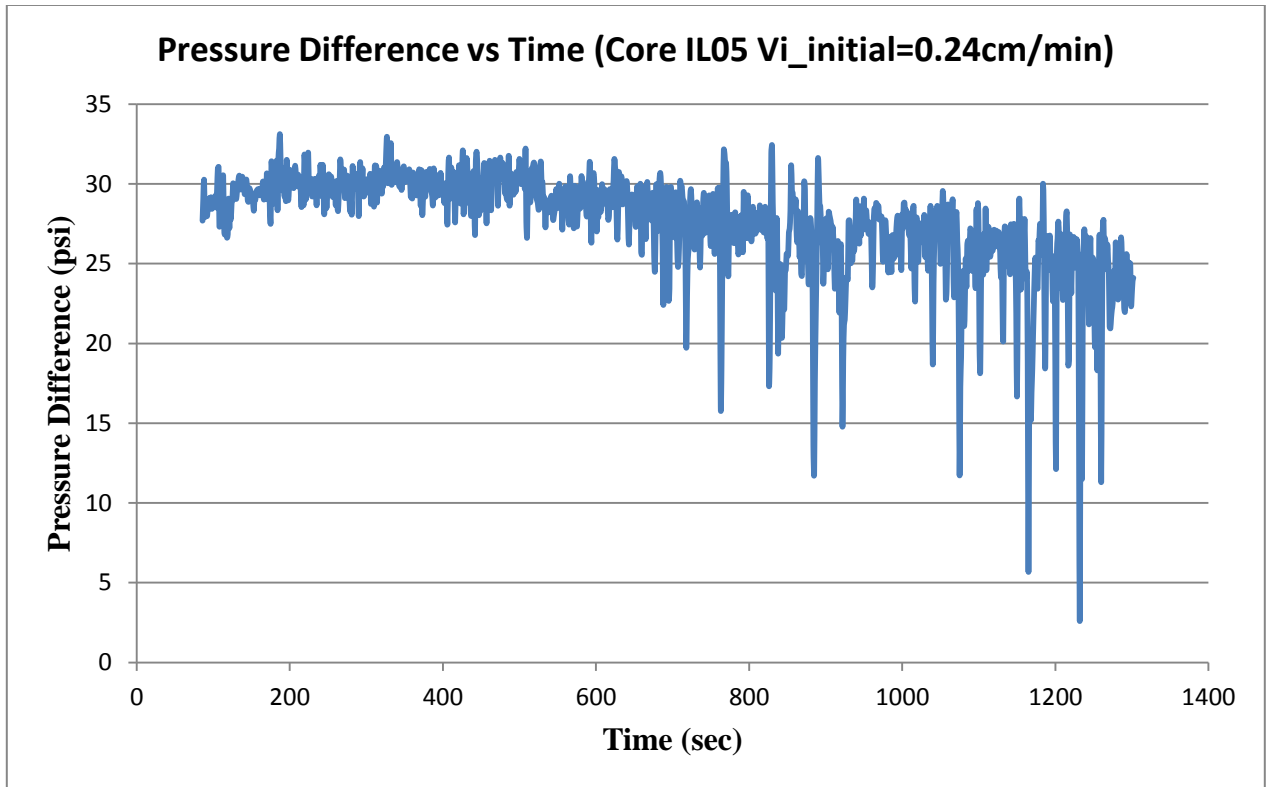


**Figure 28: Pressure Difference Observed during Acid Jetting of Core IL05 for 20minutes with No Breakthrough at Injection Velocity of 150 ft/s**

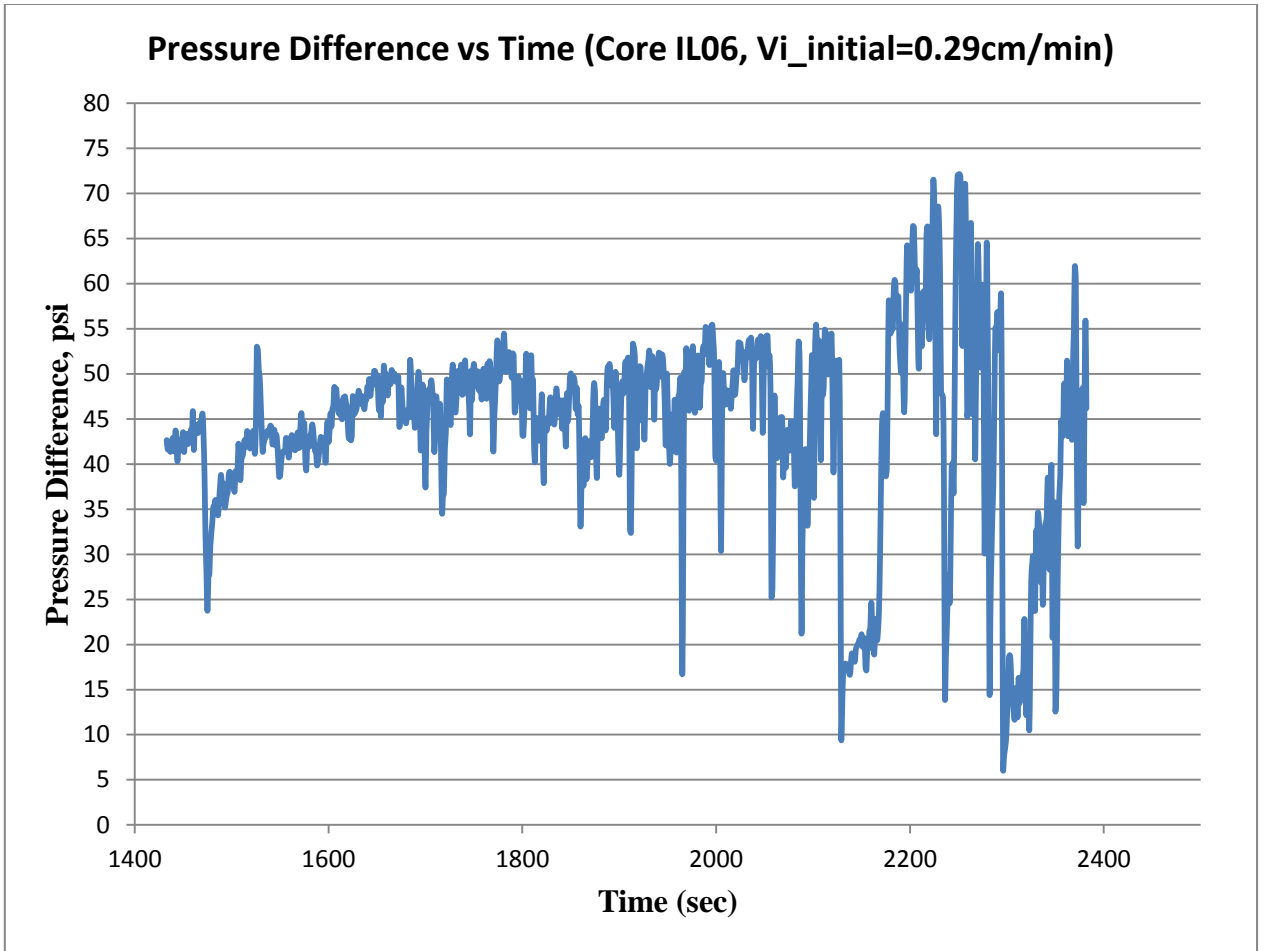


**Figure 29: Pressure Difference Observed during Acid Jetting of Core IL06 for 15minutes until Breakthrough at Injection Velocity of 150 ft/s**

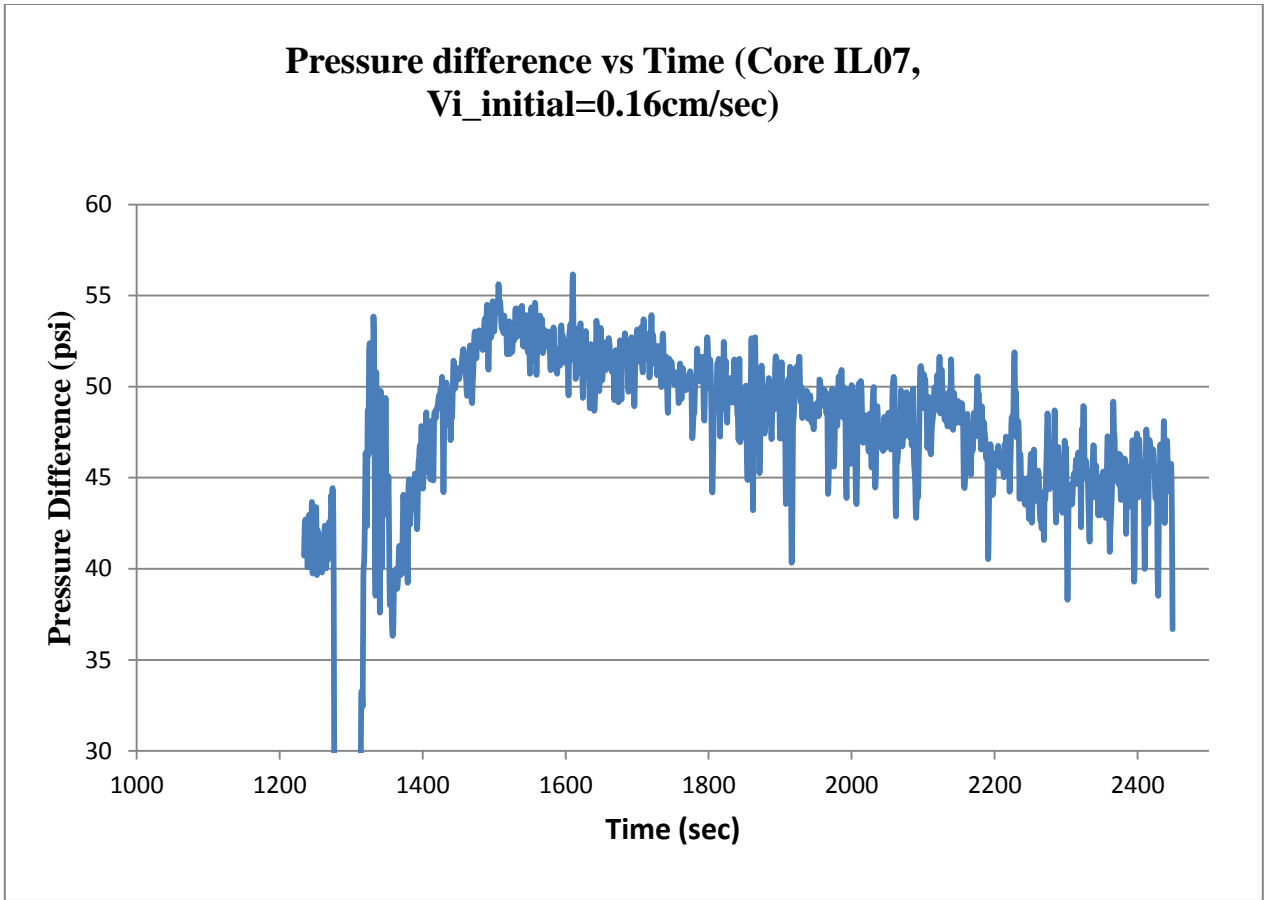


**Figure 30: Pressure Difference Observed during Acid Jetting of Core IL07 for 20minutes with No Breakthrough at Injection Velocity of 107ft/sec**

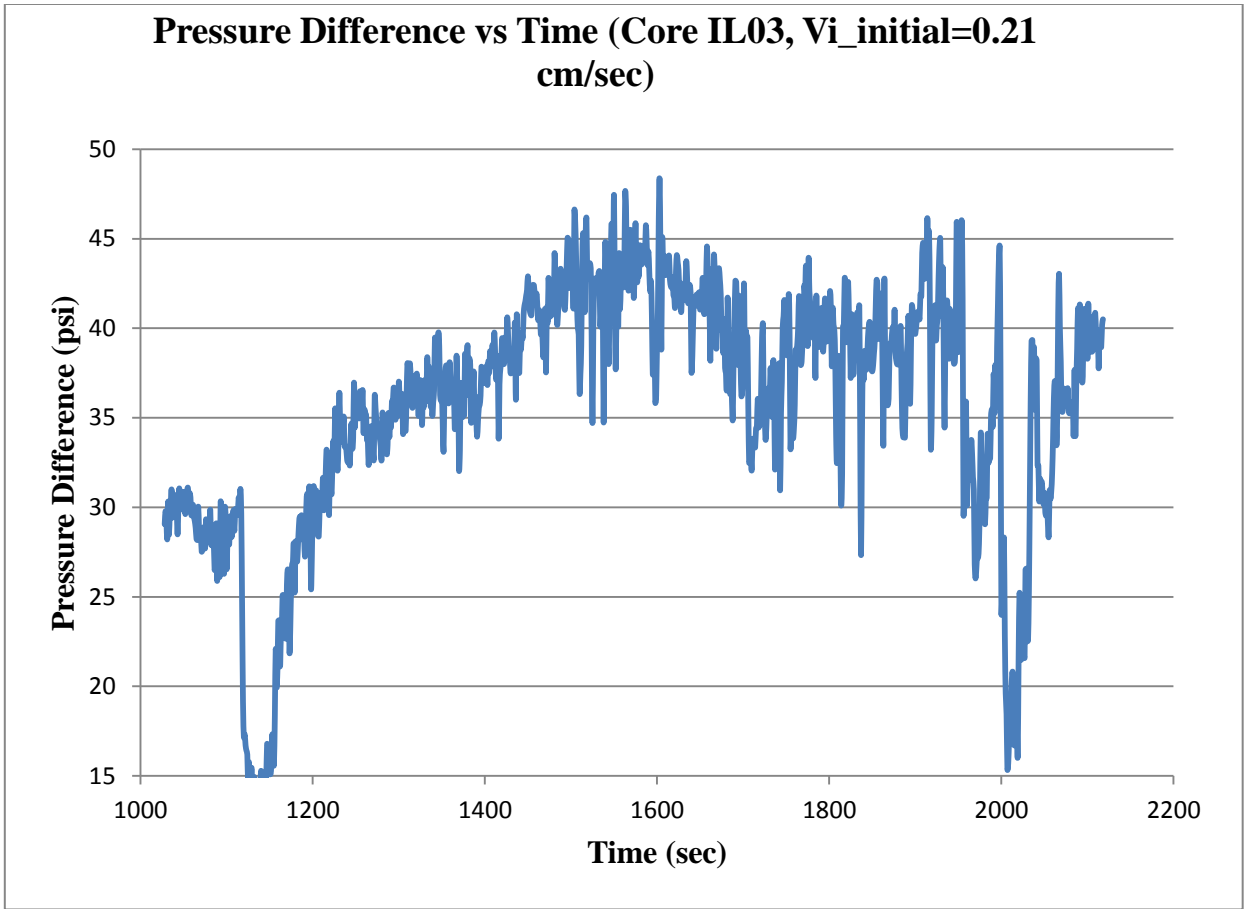


**Figure 31: Pressure Difference Observed during Acid Jetting of Core IL03 for 17minutes until Breakthrough at Injection Velocity of 107ft/sec**

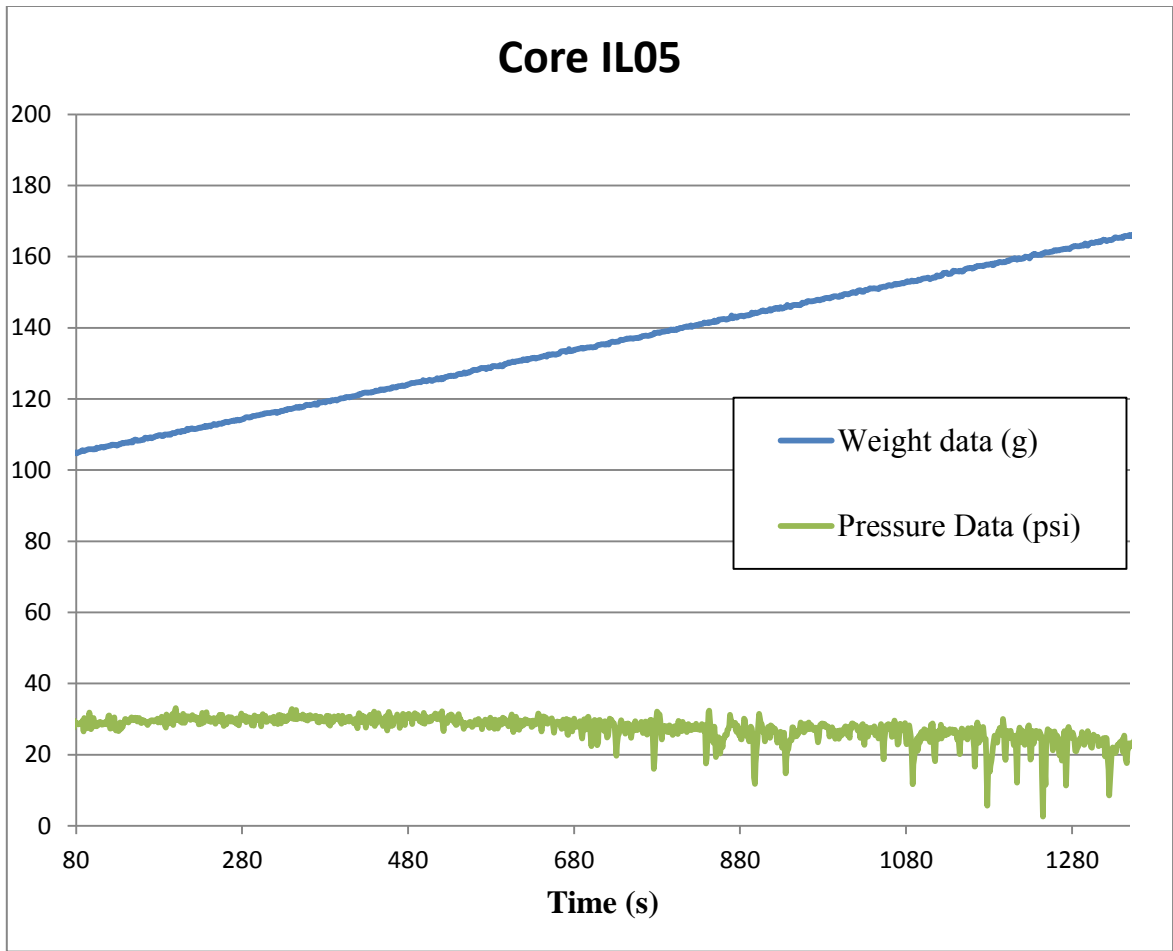


**Figure 32: Weight and Pressure Data during Acid Jetting of Core IL05**

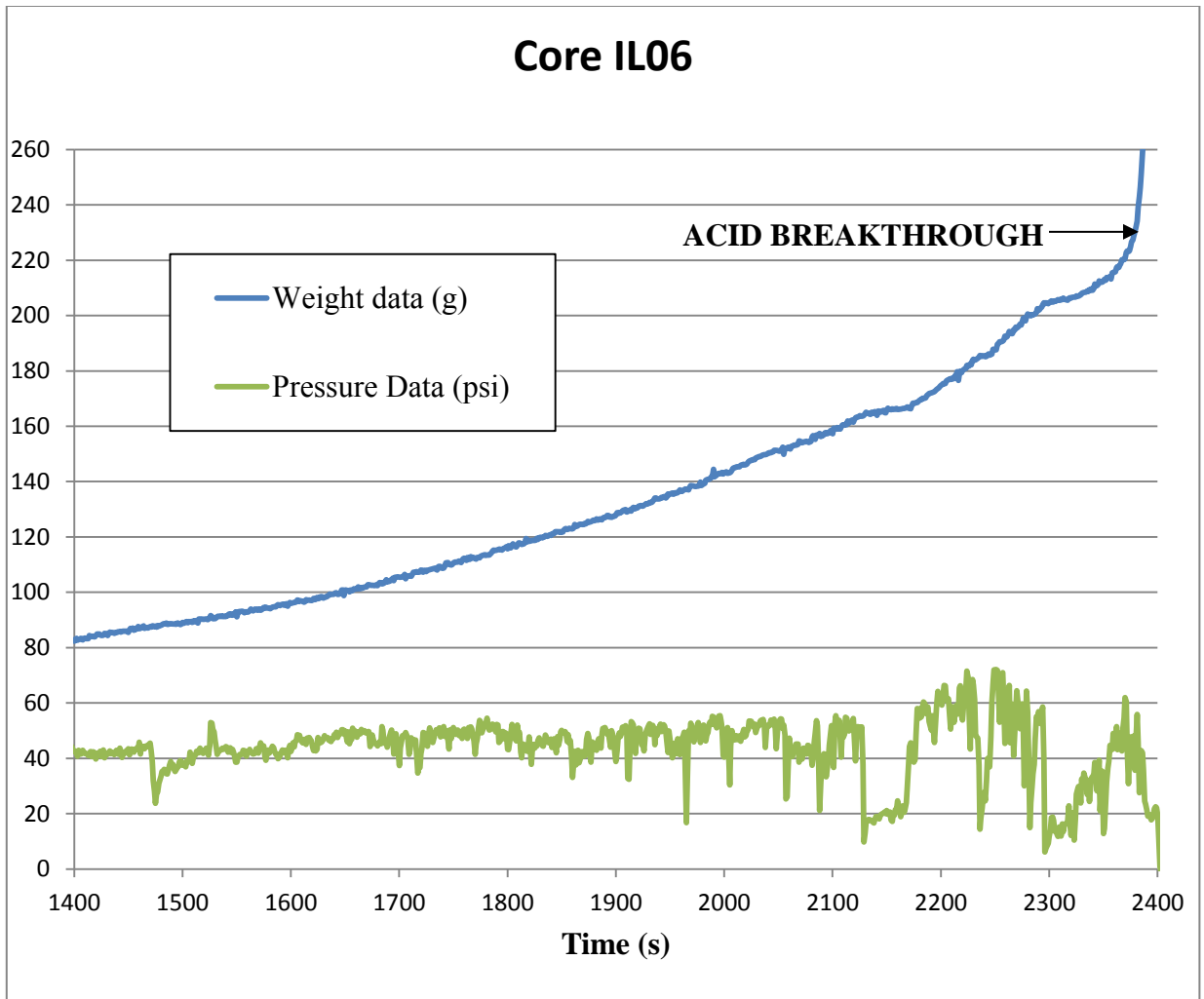


**Figure 33: Weight and Pressure Data during Acid Jetting of Core IL06**

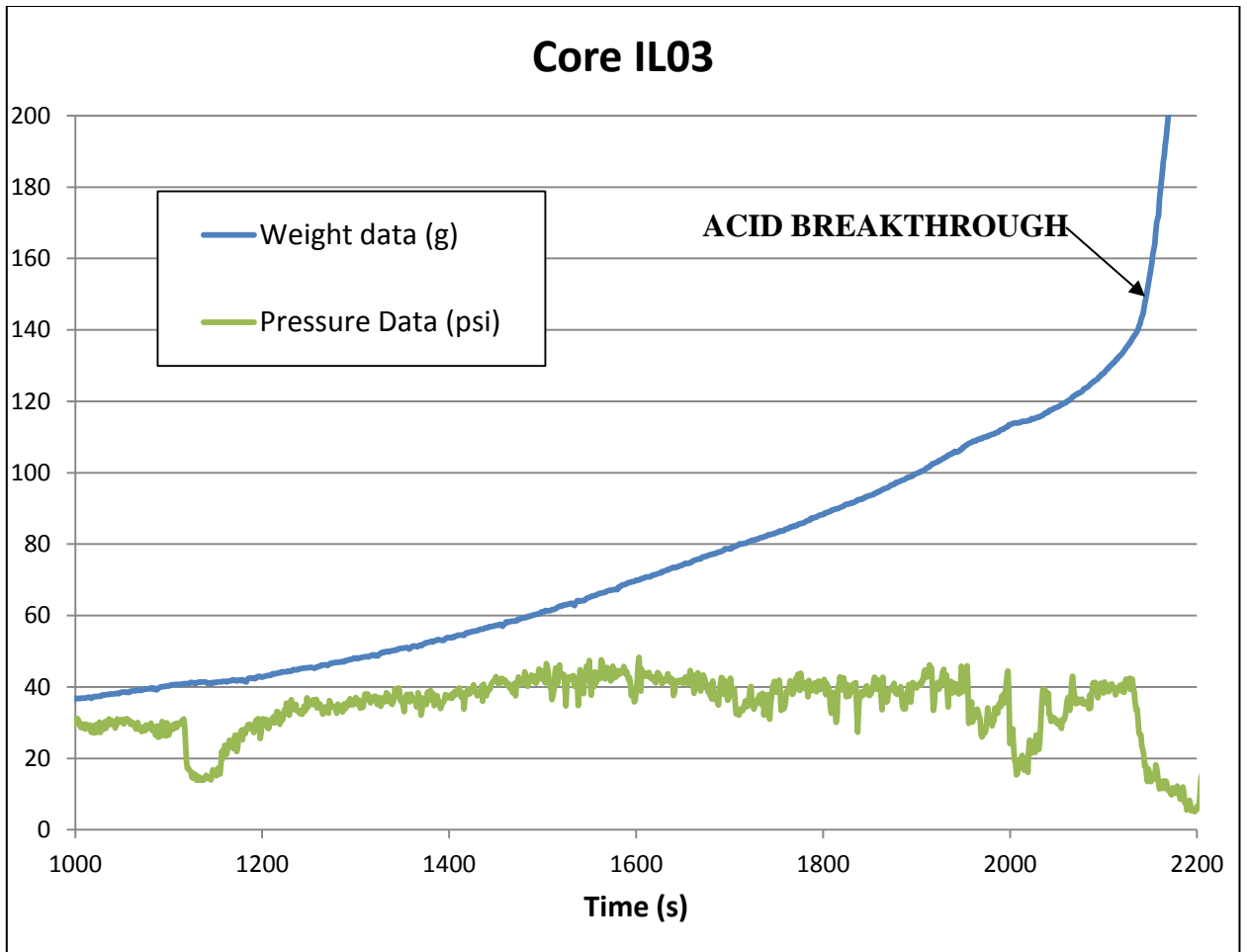


**Figure 34: Weight and Pressure Data during Acid Jetting of Core IL03**



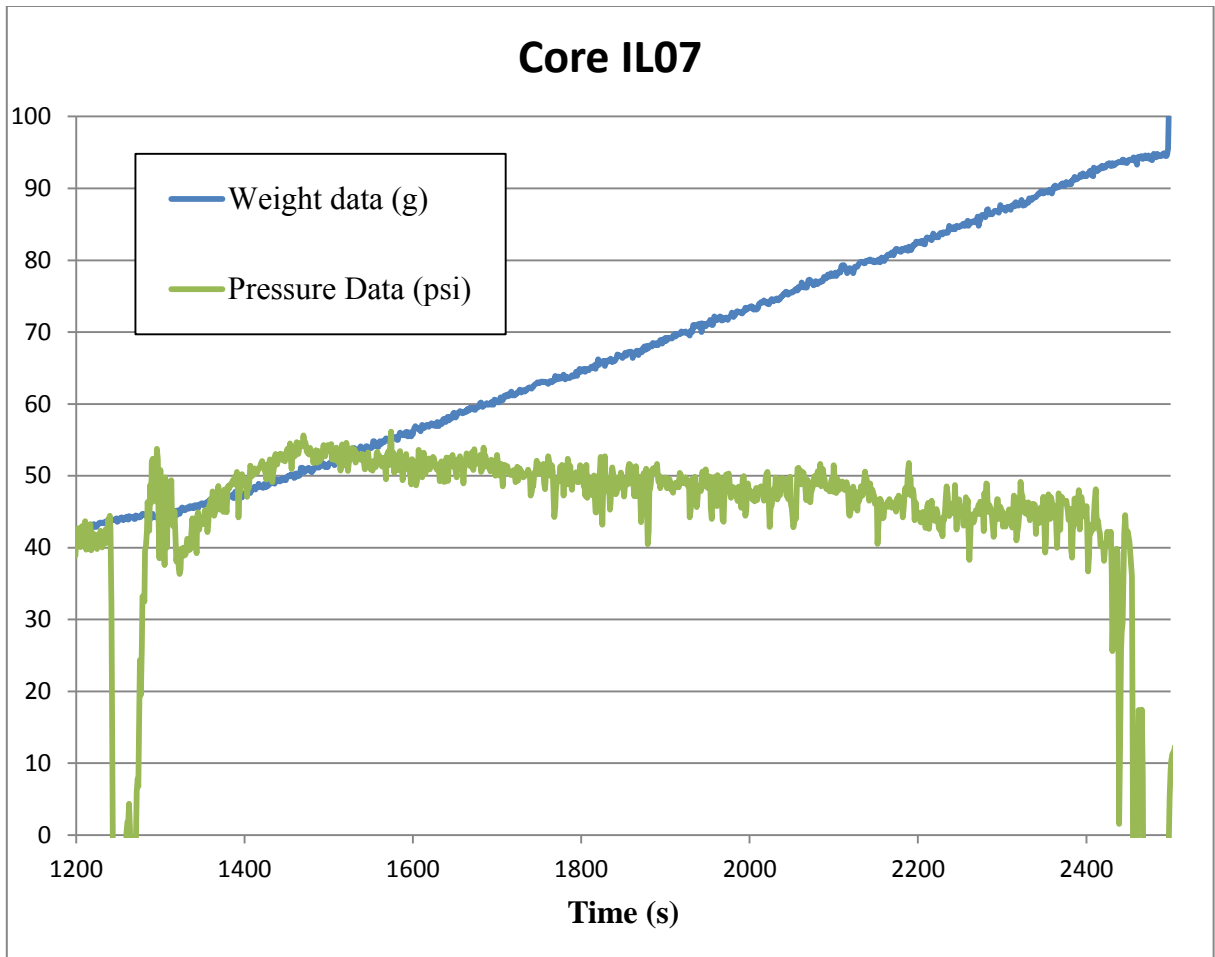


**Figure 35: Weight and Pressure Data during Acid Jetting of Core IL07**

APPENDIX B  
CORE IMAGES

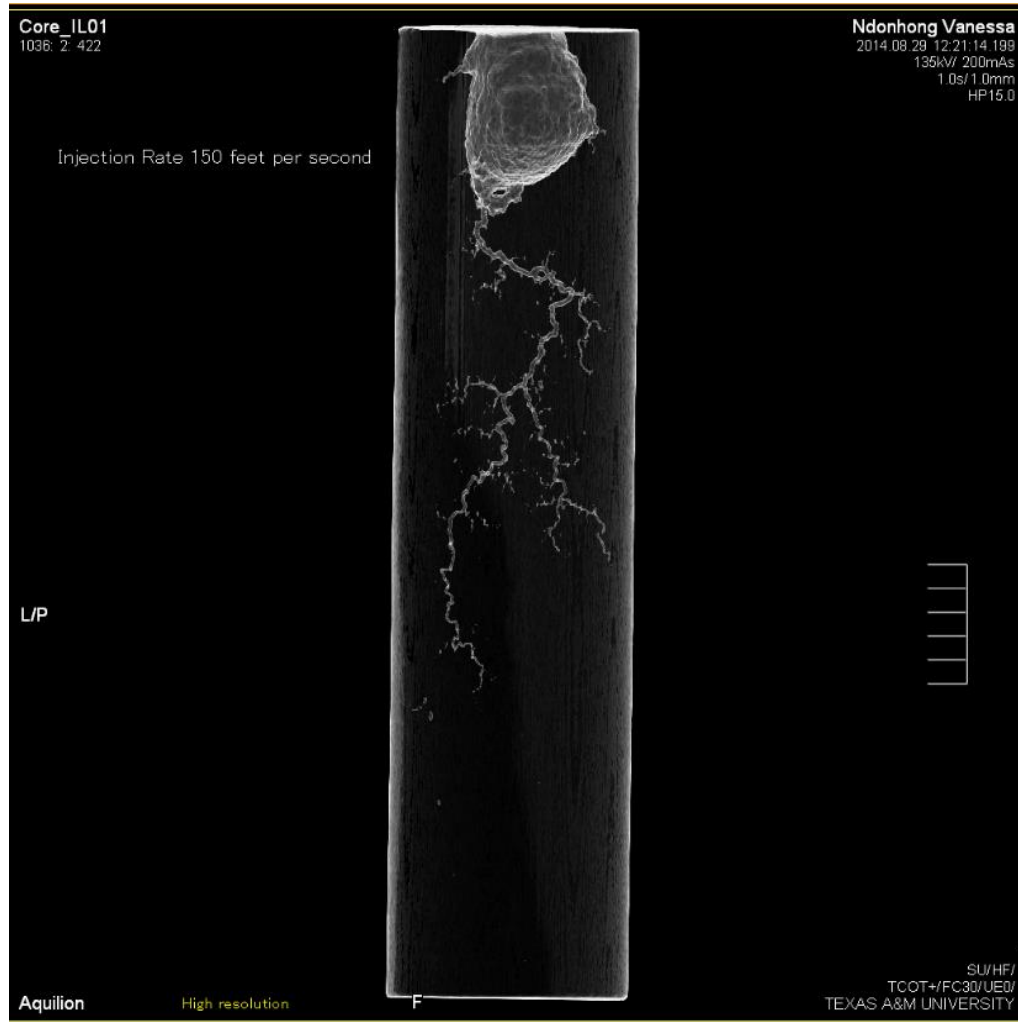
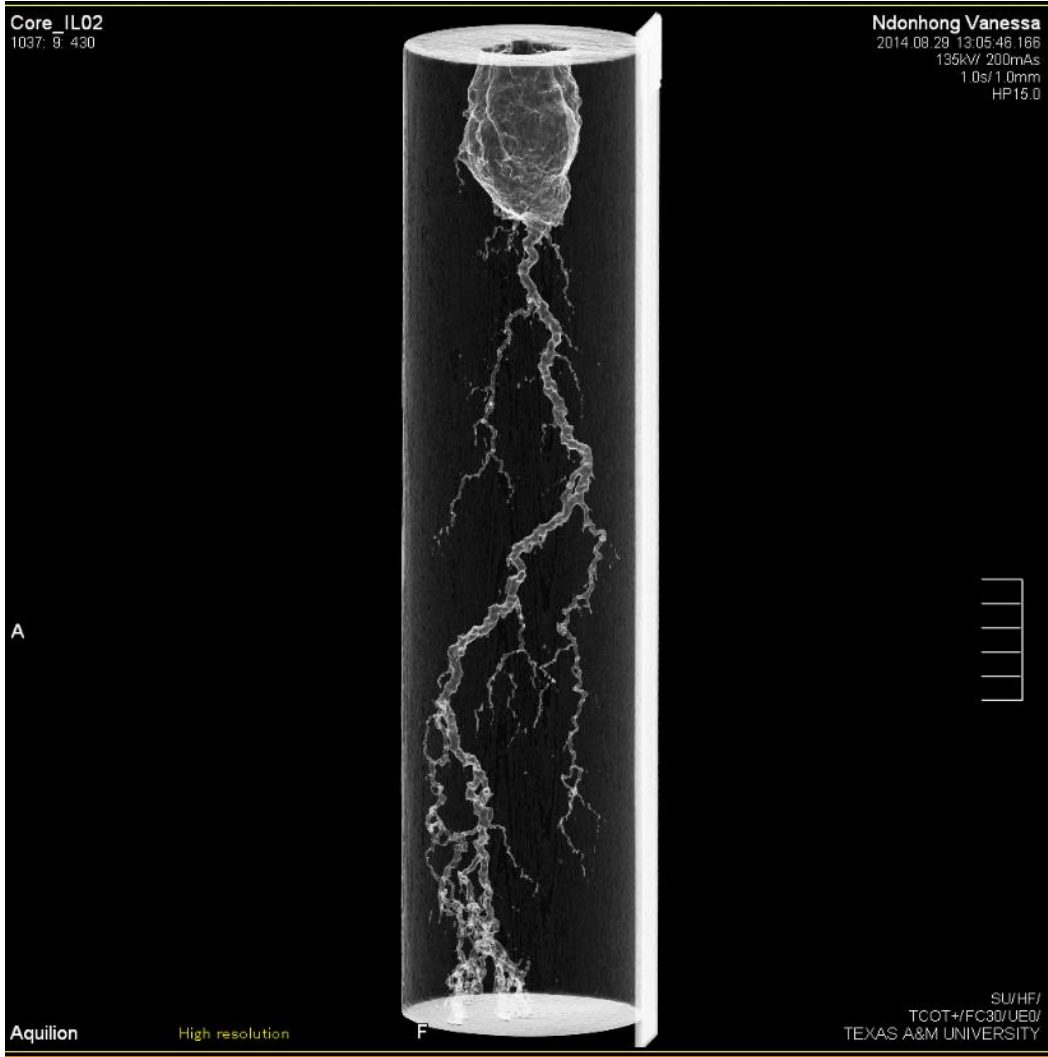
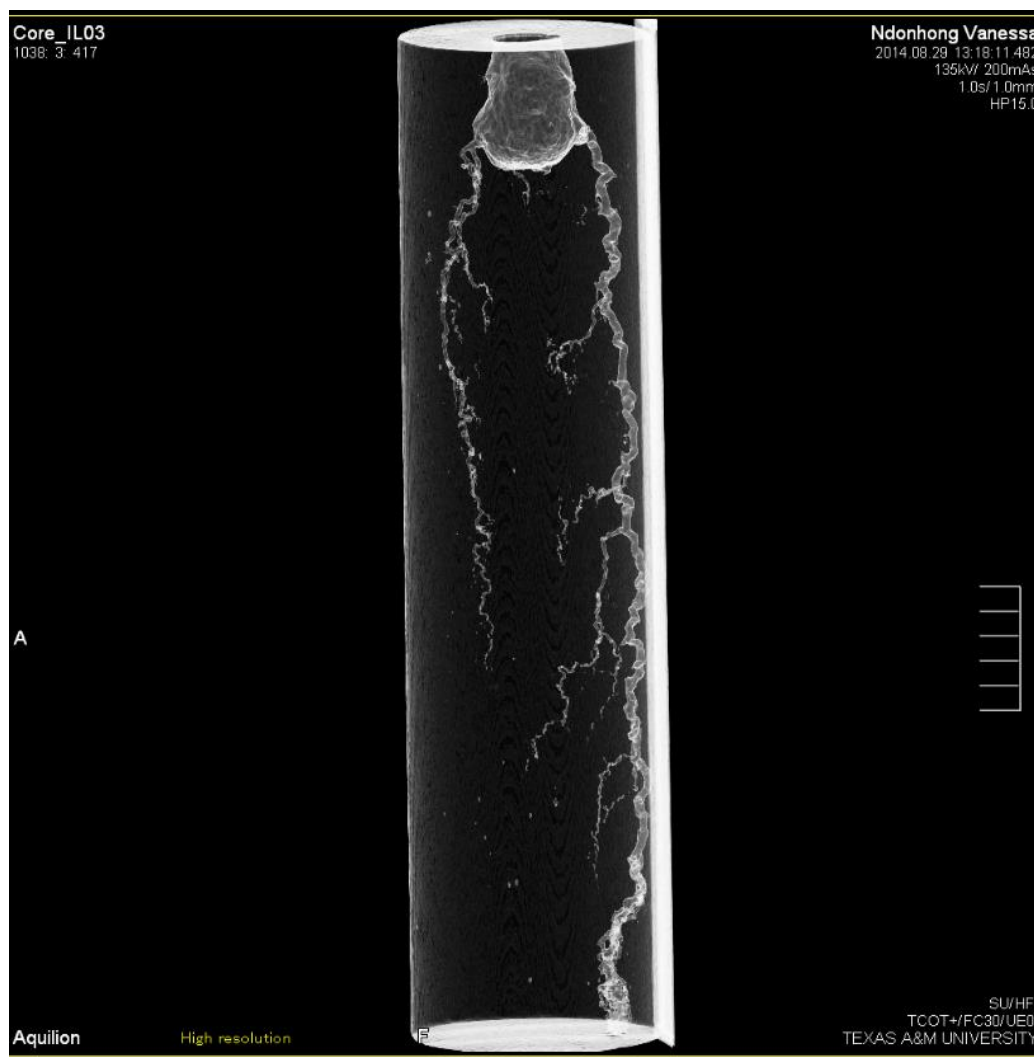


Figure 36: Core IL01 CT Scan after Acid Jetting



**Figure 37: Core IL02 CT Scan after Acid Jetting**



**Figure 38: Core IL03 CT Scan after Acid Jetting**

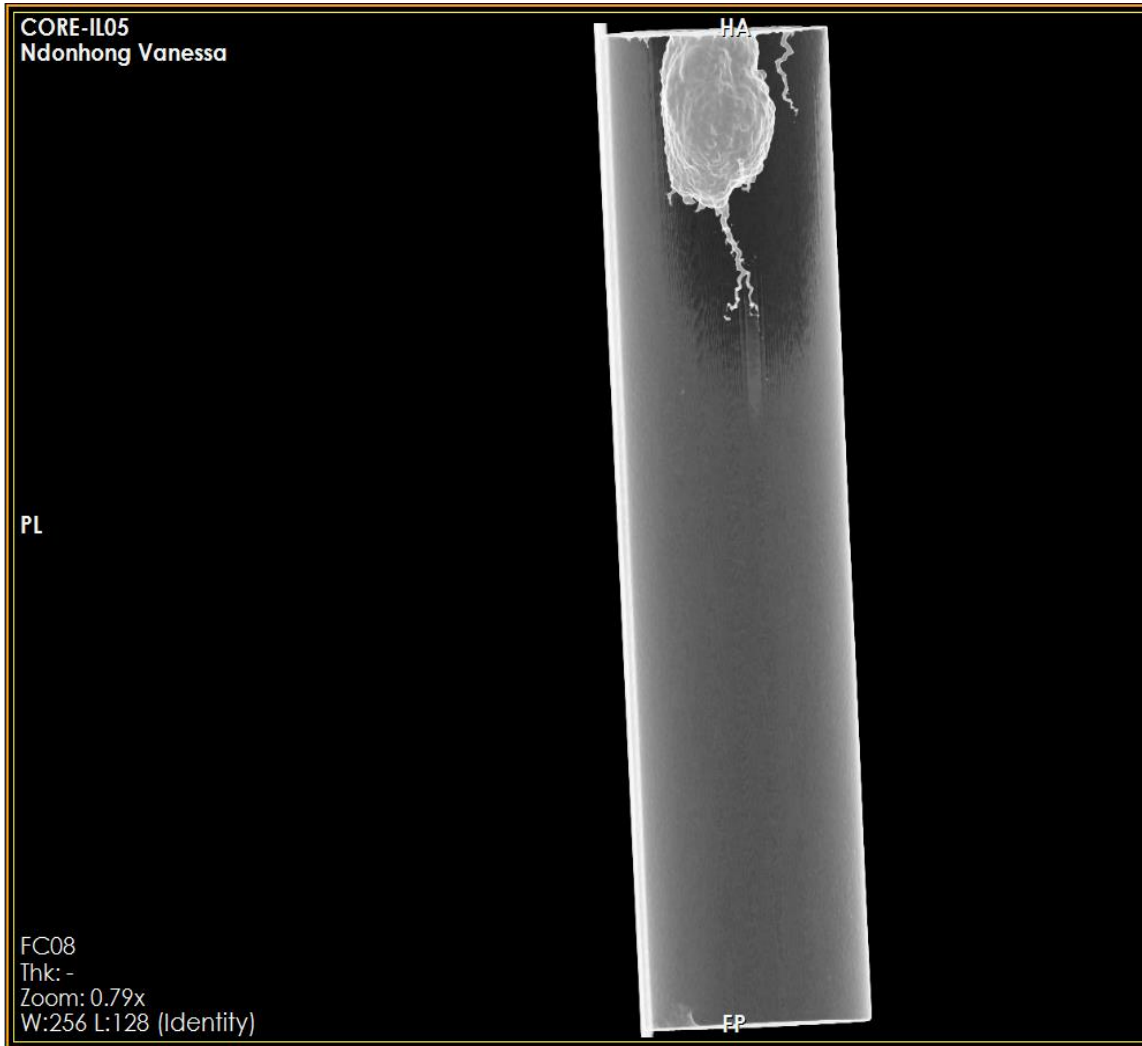


**Figure 39: Core IL05 CT Scan after Acid Jetting**

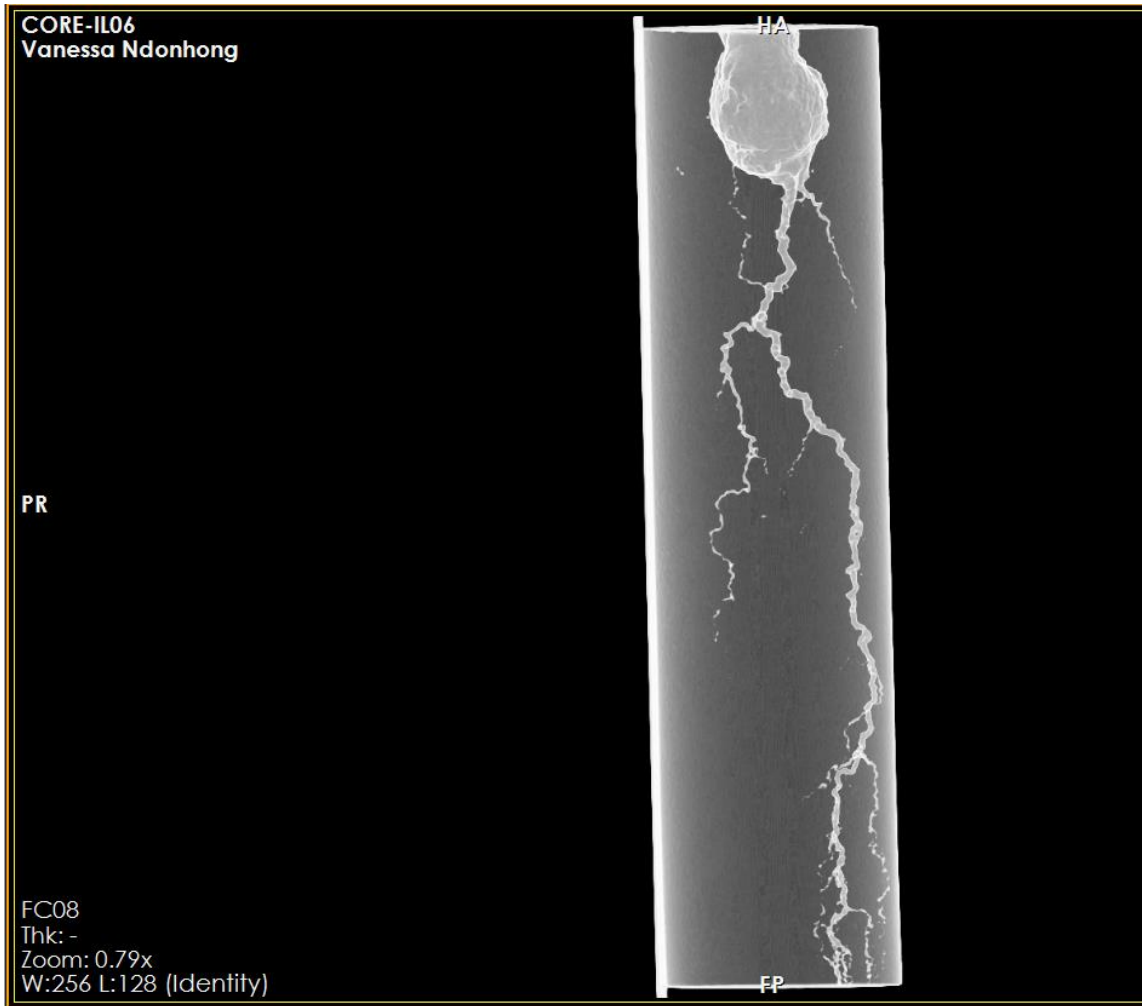


**Figure 40: Core IL06 CT Scan after Acid Jetting**

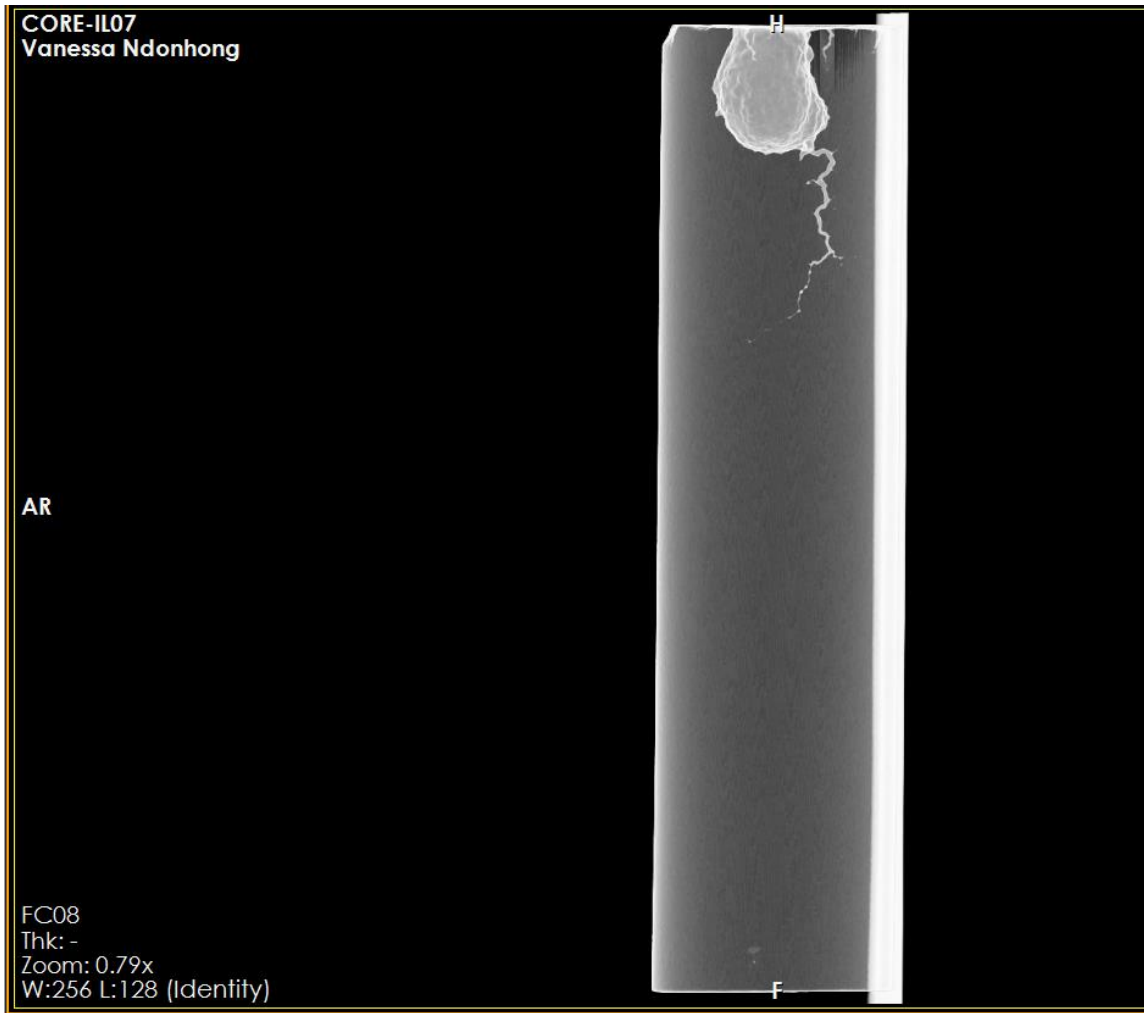


**Figure 41: Core IL07 CT Scan after Acid Jetting**

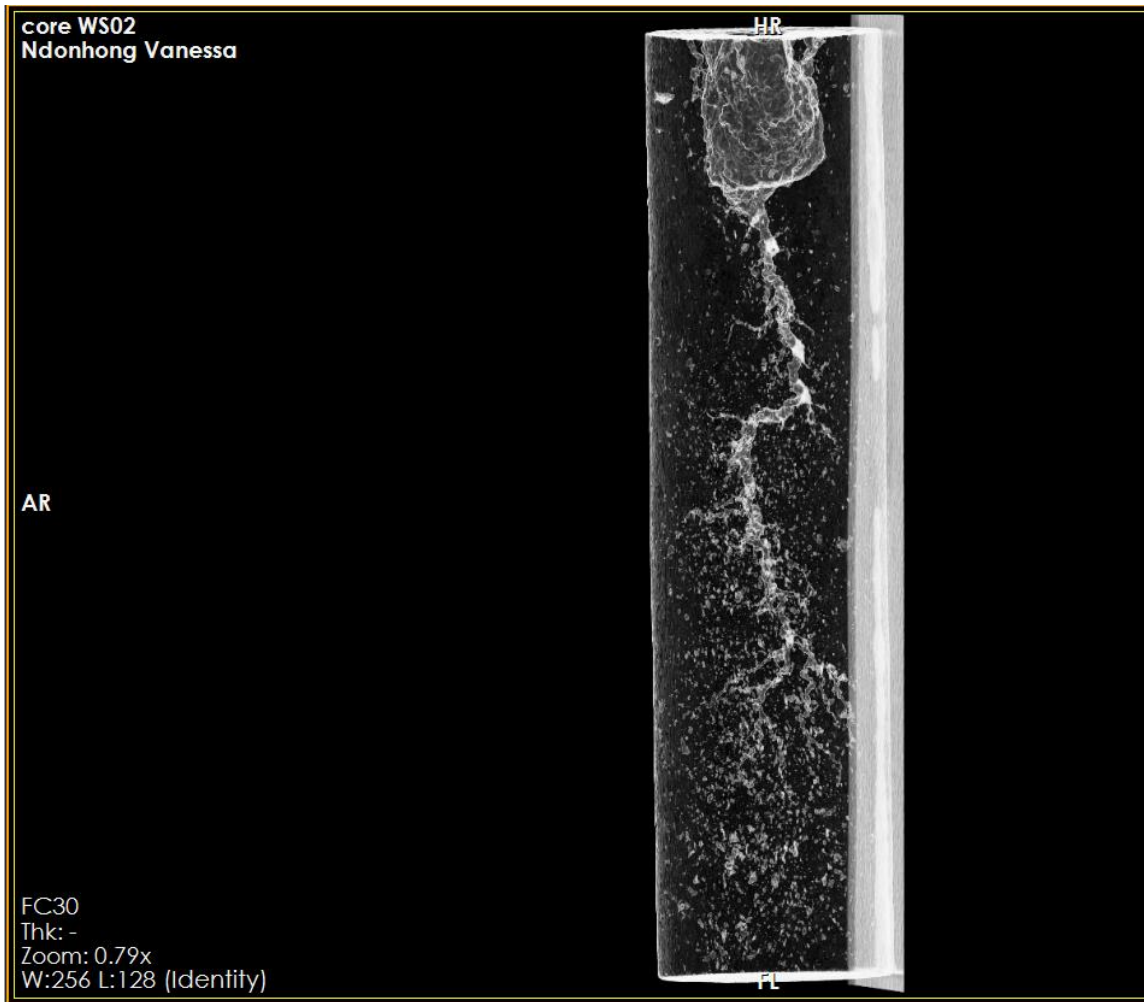


**Figure 42: Core WS02 CT Scan after Acid Jetting**



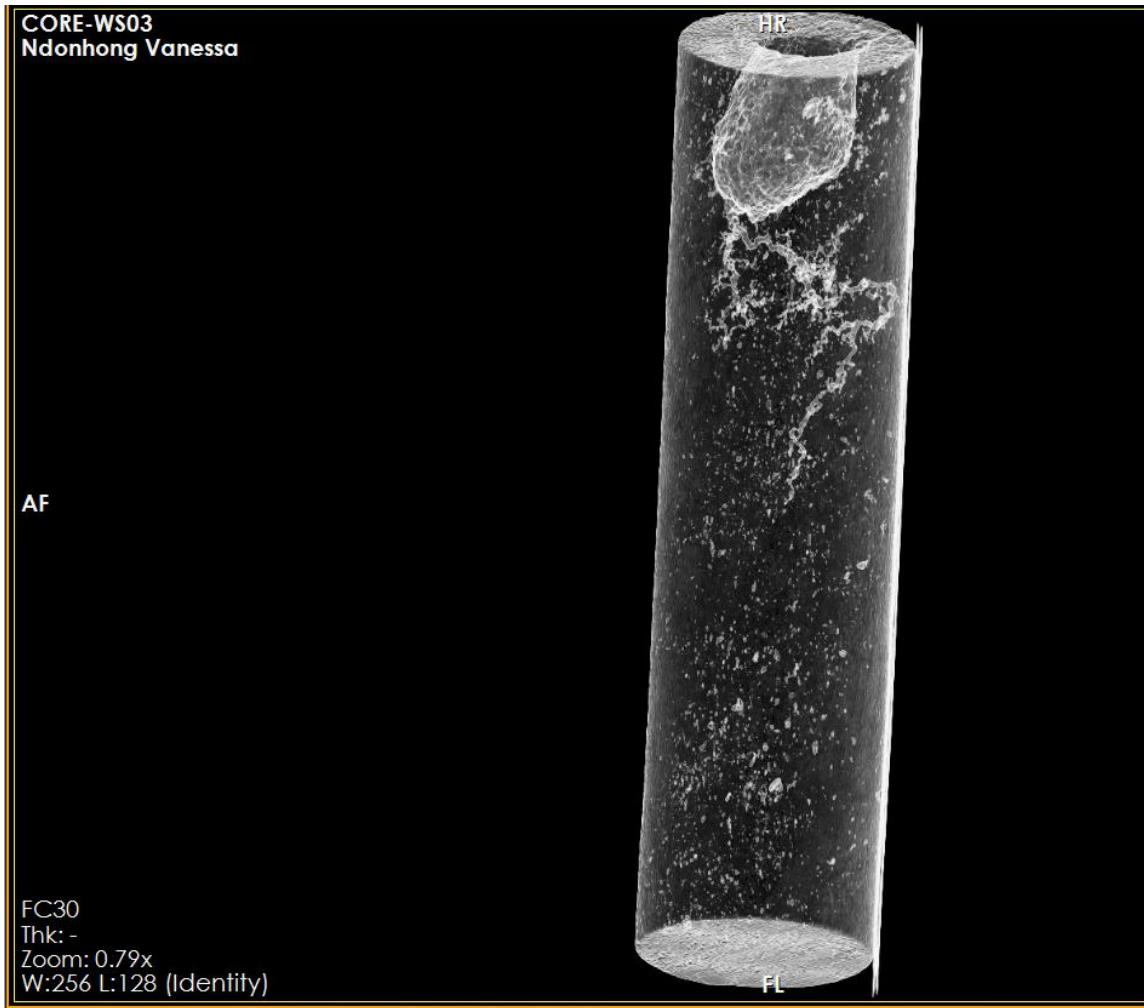


**Figure 43: Core WS03 CT Scan after Acid Jetting**



**Figure 44: Core WS04 CT Scan after Acid Jetting**